



Ricerca di Sistema elettrico

# Development and Application of Monte Carlo Neutronics Methodologies for Safety Studies of Current Operating Reactors

Kenneth W. Burn, Patrizio Console Camprini

DEVELOPMENT AND APPLICATION OF MONTE CARLO NEUTRONICS METHODOLOGIES FOR SAFETY STUDIES OF  
CURRENT OPERATING REACTORS

Kenneth W. Burn, Patrizio Console Camprini - ENEA

Settembre 2016

Report Ricerca di Sistema Elettrico

Accordo di Programma Ministero dello Sviluppo Economico - ENEA

Piano Annuale di Realizzazione 2015

Area: Produzione di energia elettrica e protezione dell'ambiente

Progetto: Sviluppo competenze scientifiche nel campo della sicurezza nucleare e collaborazione ai programmi internazionali per il nucleare di IV Generazione

Obiettivo: Sviluppo competenze scientifiche nel campo della sicurezza nucleare

Responsabile del Progetto: Felice De Rosa, ENEA

**Title**

**Development and Application of  
 Monte Carlo Neutronics Methodologies for Safety Studies  
 of Current Operating Reactors**  
**(Analisi neutronica con Metodi Monte Carlo di Impianti Nucleari Tipo PWR)**

**Descrittori**
**Tipologia del documento:** Rapporto Tecnico

**Collocazione contrattuale:** Accordo di Programma ENEA-MSE su sicurezza nucleare e reattori di IV generazione

**Argomenti trattati:** Metodi Monte Carlo  
 Neutronica  
 Reattori Nucleari Evolutivi  
 Tecniche Riduzione della Varianza

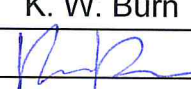
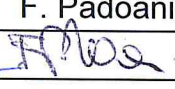
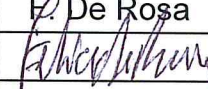
**Sommario**

Within the framework of safety analysis of currently operated nuclear power reactors, innovative Monte Carlo methods have been developed to perform both fixed source and eigenvalue simulations; taking advantage of variance reduction techniques for in-core and ex-core responses. The activity is carried out within the present work, dealing with a benchmarking with two different nuclear systems. A close collaboration is carried on with IRSN (French Institute for Radiation Protection and Nuclear Safety). In fact, two complementary sample problems were adopted: TAPIRO, a small fast research reactor and the large GEN-III PWR model employed before the TIHANGE model for the calculation of neutron and gamma detectors in and outside the pressure vessel well. The TAPIRO model provided a good benchmark, while Tihange offered a case study for ex-core detector analysis through the deep shield in the reactor well. First approach has been eigenvalue calculation during which the fission source is sampled and then wrote to a file. Secondly, DSA is employed in fixed source simulation. In addition, in-core or ex-core local responses are added to in-core global responses to utilize DSA variance reduction technique directly in an eigenvalue simulation – thanks to the multi-response capability. Finally, a simple experimental benchmark is used to check nuclear data utilized and methodology consistency: PCA-Replica is selected for this purpose.

**Note**

Il presente rapporto è stato prodotto con il contributo di:  
 Kenneth W. Burn (ENEA), Patrizio Console Camprini (ENEA)

**Copia n.**
**In carico a:**

2			NOME			
			FIRMA			
1			NOME			
			FIRMA			
0	EMISSIONE	21/09/2016	NOME	K. W. Burn	F. Padoani	F. De Rosa
			FIRMA			
REV.	DESCRIZIONE	DATA		REDAZIONE	CONVALIDA	APPROVAZIONE

 <b>Ricerca Sistema Elettrico</b>	<b>Sigla di identificazione</b>	<b>Rev.</b>	<b>Distrib.</b>	<b>Pag.</b>	<b>di</b>
	<b>ADPFISS-LP1-079</b>	0	L	2	45

## 1. INTRODUCTION

Dealing as it does with current operating reactors, this activity is carried out in close collaboration with IRSN (L'Institut de Radioprotection et de Sûreté Nucléaire), France. The collaboration has been ongoing for nearly six years and may be divided chronologically as follows:

- 1) Evaluation of the effect of a heavy steel reflector of a GEN-III PWR design on the signal in the ex-core neutron detectors in the pressure vessel well;
- 2) Analysis of the phenomenon of “flux tilt” in a GEN-III PWR design and its possible magnification due to a heavy steel reflector;
- 3) Calculation of the responses of a range of neutron and gamma detectors, present for additional safety requirements, placed in the pressure vessel well and within the concrete surrounding the well. This was done both for the above GEN-III PWR design and for a GEN-II PWR model (TIHANGE in Belgium).

In support of the above applications there is an ongoing activity of development of Monte Carlo methodology. This has focused in the last years on applying variance reduction techniques to the source-iteration algorithm solution of the eigenvalue problem. The immediate application of this development is to avoid the necessity of decoupling when calculating ex-core responses.

The period covered by the current report (Sept. 2015 – Sept. 2016) covers the latter part of point 3) above (responses of ex-core neutron and gamma detectors placed in the pressure vessel well and in the surrounding concrete of TIHANGE). Furthermore, during this period there was an important didactic element epitomized by a 4-day course on advanced variance reduction techniques in Monte Carlo, held at IRSN in May, 2016. (A copy of this course is available on request.)


There are two external publications covering much of the work in the period in question:

K.W. Burn, P. Console Camprini, “Radiation transport out from the reactor core: to decouple or not to decouple”, Proc. Int. Conf. Rad. Shielding (ICRS-13), Paris, Oct. 3-6, 2016

M. Brovchenko, B. Dechenaux, K.W. Burn, P. Console Camprini, I. Duhamel, A. Peron: “Neutron-gamma flux and dose calculations in a Pressurized Water Reactor (PWR)”, Proc. Int. Conf. Rad. Shielding (ICRS-13), Paris, Oct. 3-6, 2016


These papers are not attached for copyright reasons but will appear in the proceedings of the International Conference of Radiation Shielding, ICRS-13, Paris, Oct. 2016.

This report is divided into the following sections: a summary of methodological developments relevant to such PWR applications; a short account of the TIHANGE calculations; the TAPIRO calculations (TAPIRO has been proposed to be employed for actinide cross-section measurements) - although this is a small, fast, core it is useful as a benchmark for the application of variance reduction techniques to the source-iteration algorithm solution of the eigenvalue problem; the ongoing PCA Replica experimental benchmark calculations.

 <b>Ricerca Sistema Elettrico</b>	<b>Sigla di identificazione</b>	<b>Rev.</b>	<b>Distrib.</b>	<b>Pag.</b>	<b>di</b>
	<b>ADPFISS-LP1-079</b>	0	L	3	45

The Monte Carlo vehicle employed was MCNP, either version 5.1.4 [1] or version 6.1 [2]. The variance reduction technique was the DSA, for fixed sources [3] and for eigenvalue problems [4-6], both modes employing version 5.1.4 of MCNP as a vehicle. (Having generated variance reduction parameters, they were then converted to a weight window and run with MCNP 6.1.)

The computing resources and the related technical support used for this work have been provided by CRESCO/ENEAGRID High Performance Computing infrastructure and its staff. CRESCO/ENEAGRID High Performance Computing infrastructure is funded by ENEA, the Italian National Agency for New Technologies, Energy and Sustainable Economic Development and by Italian and European research programmes, see <http://www.cresco.enea.it/english> for information. [7]

 <b>Ricerca Sistema Elettrico</b>	<b>Sigla di identificazione</b>	<b>Rev.</b>	<b>Distrib.</b>	<b>Pag.</b>	<b>di</b>
	<b>ADPFISS-LP1-079</b>	0	L	4	45

## **SUMMARY OF METHODOLOGICAL DEVELOPMENTS**

Further benchmarking of the technique described in [4-6] focusing on ex-core responses was carried out. Two complementary sample problems were adopted: TAPIRO, a small fast research reactor and the large GEN-III PWR model employed before the TIHANGE model for the calculation of neutron and gamma detectors in and outside the pressure vessel well.

The TAPIRO model provided a good benchmark. Superhistories of one fission neutron generation were sufficient and the results with the decoupled and single calculation approaches were consistent. Instead the PWR model did not maintain the fundamental mode with one fission neutron generation per superhistory. Superhistories of 10 or more fission generations however did maintain the fundamental mode. Further details are provided in the Appendix in presentational form and in the first ICRS-13 paper mentioned in the Introduction.

## 2. TIHANGE CALCULATIONS

The calculation was decoupled in a standard fashion into an eigenvalue part that wrote the fission source and a fixed source part that read the same source and ran out from the core. The fixed source part included variance reduction. The source was defined for each fuel pin over a whole 360° azimuthal segment and with 21 axial segments. Given space limitations, 3 calculations were required (with identical tracks but different tallies) to write the source.

Such a pin-by-pin source could not be read by standard MCNP and required an in-house MCNP patch. The rest of the calculational sequence is reasonably standard. Neutron and gamma responses were requested radially, between the pressure vessel and the concrete and at various depths in the side concrete, and axially, on the lower surface of the pressure vessel, on the surface of the concrete at the bottom of the well and at various depths in the concrete at the bottom of the well. After pruning the total number of requested responses to 50 (36 neutron and 14 gamma), variance reduction parameters were generated for all the neutron and gamma responses in a single run using the multi-response capability [3].

The following figures show some cross-sections of the MCNP model:

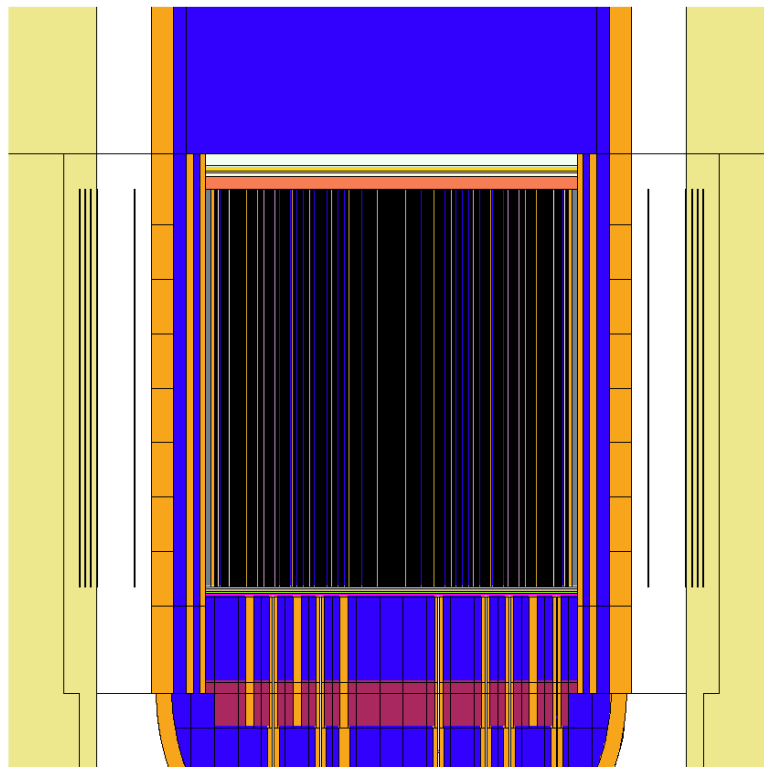


Figure 2.1 - Axial cross-section centred at the core mid-plane (width of figure: 7m)

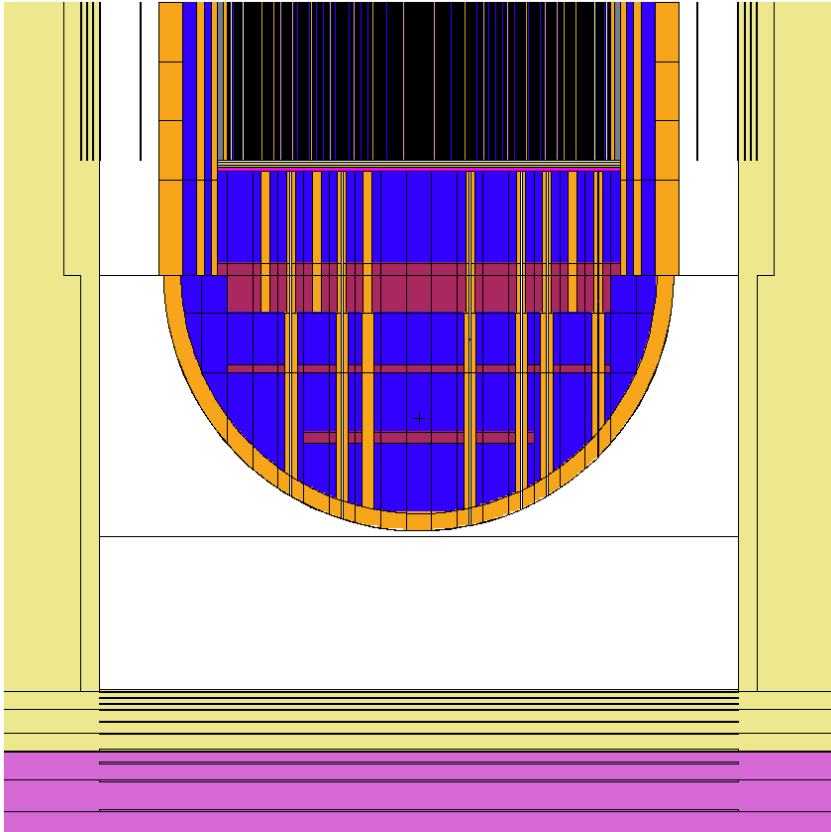


Figure 2.2 - Axial cross-section centred at 4m below the core mid-plane (width of figure: 7m)

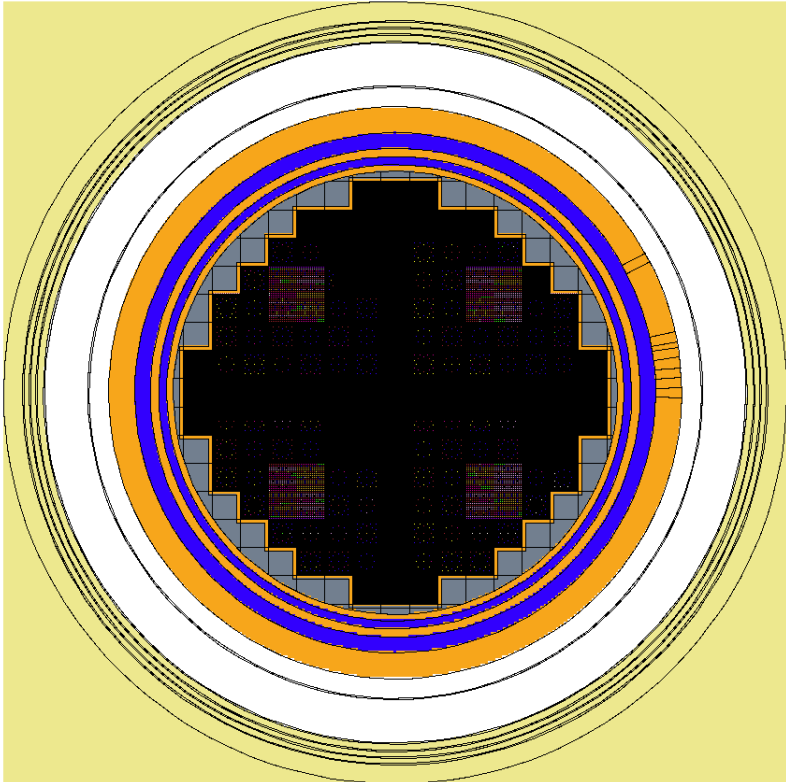


Figure 2.3 - Radial cross-section at the core mid-plane (width of figure: 6m)



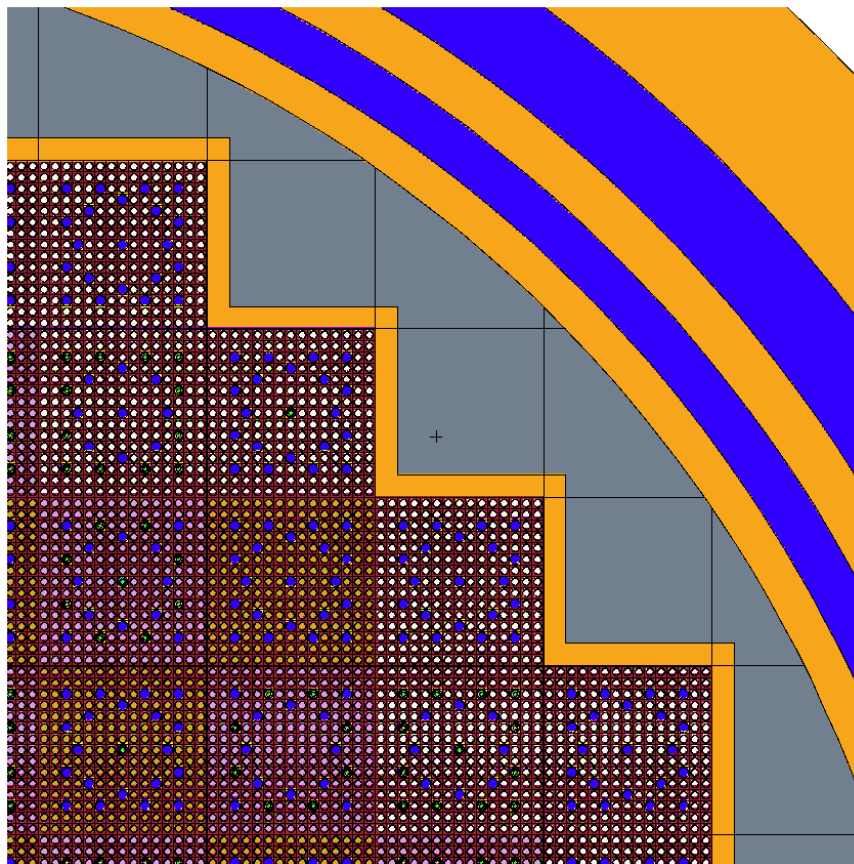


Figure 2.4 - Radial cross-section at the core mid-plane showing detail at edge of core (width of figure: 1.1m)

Further details of this study may be found in: M. Brovchenko, B. Dechenaux, K.W. Burn, P. Console Camprini, I. Duhamel, A. Peron “Neutron-gamma flux and dose calculations in a Pressurized Water Reactor (PWR)”, Proc. Int. Conf. Rad. Shielding (ICRS-13), Paris, Oct. 3-6, 2016.

The responses in the calculations up to this point had all been azimuthally averaged. A second series of calculations were then made employing detectors that were at given azimuthal positions. Firstly, a single neutron detector was studied, then 10 neutron and gamma detectors at 5 different positions. These calculations were intended more as a benchmark for variance reduction techniques and some comparisons with the weight window generator in MCNP were made. Further details may be found in [8].

### 3. SIMULATIONS FOR TAPIRO REACTOR

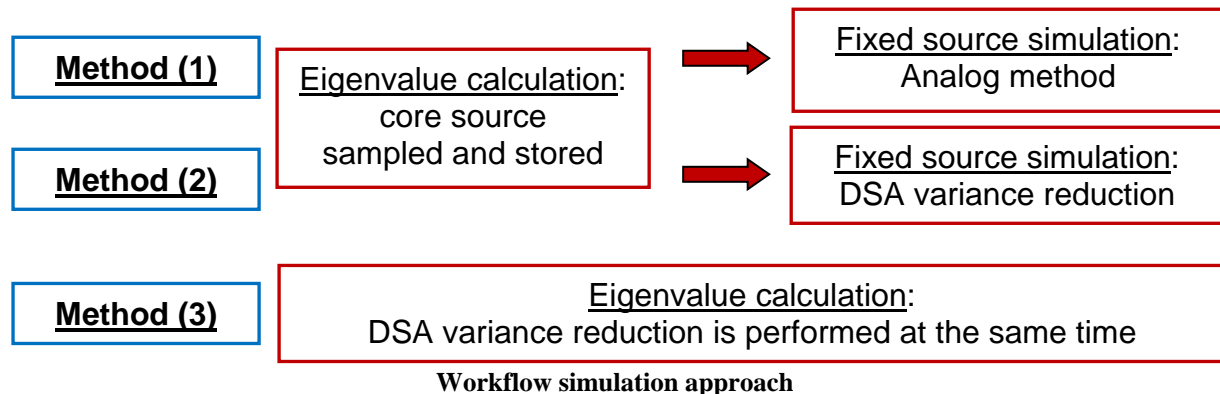
Within the framework of the activities concerning the methodological comparison between fixed source and eigenvalue calculations for ex-core response, a fast-spectrum and geometrically small nuclear system has been analysed.

The present study offers particular ex-core evaluations aiming at preliminary simulations of some irradiation campaigns for Minor Actinides in the TAPIRO research reactor. Efforts have been conducted on MAs transmutation study, mainly about nuclear data, due to the poor knowledge in this field. Several NEA and IAEA Working Groups addressed these issues, even recommending integral measurements, complementary to parallel efforts for differential measurements, for the several nuclides of MAs from viewpoints of design of transmutation systems and of fuel cycle. In the framework of one of the NEA Expert Group on Integral Experiments for Minor Actinide Management (EGIEMAM) [9] the feasibility of MAs irradiation campaign in TAPIRO research reactor is carried out in this report.

Thus, results are obtained and compared, according to following methods:

1. standard eigenvalue simulation followed by a decoupled analog fixed source calculation
2. standard eigenvalue simulation followed by a fixed source calculation with DSA variance reduction tool
3. eigenvalue simulation implementing directly DSA variance reduction methodology

Graphical explanation of the workflow is reported:



#### 3.1 TAPIRO RESEARCH REACTOR

TAPIRO (TAratura Pila Rapida a potenziamento), a fast nuclear research reactor located at ENEA CASACCIA research center, was developed by ENEA, based on the project of the Argonne Fast Source Reactor (AFSR, Idaho falls). The startup was in 1971 and is currently used in supporting experimental programs finalized to [10]:

- validation of calculation codes for studies on the development of Gen-IV reactors and ADS systems
- analysis on fast neutrons damages on materials and electronics components
- training and experiences for nuclear engineering courses

In the following picture a view of TAPIRO reactor room is showed in Figure 3.1:



Figure 3.1 - TAPIRO reactor room.

It has a maximum power of 5 kW with a neutron flux of  $4 \times 10^{12} \text{ n}/(\text{cm}^2 \text{ s})$  in the centre of the core. The core is cylindrical with a diameter of about 12 cm and a similar height. It is made with metallic uranium (98.5 % uranium and 1.5 % molybdenum) with an enrichment of 93.5 % in  $^{235}\text{U}$ . It consists of 2 parts: the upper part is fixed while the lower one is movable. The core is surrounded by a double layer of copper reflector and by an external biological shield of borate concrete. It is refrigerated by helium as coolant. The reactor is equipped with 2 shim rods, 2 safety rods and a regulating rod. These rods are realized with the same material of the reflector and the reactor is controlled increasing or reducing the leaks of neutrons.

A horizontal section of the reactor at 1 m from the floor is showed in Figure 3.2:

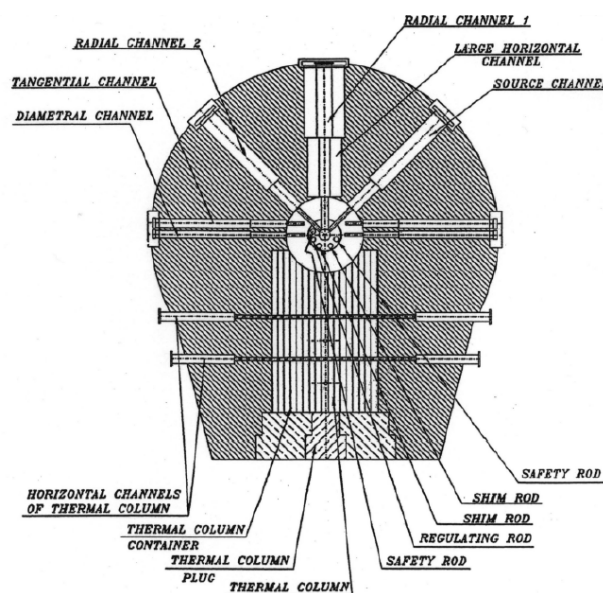


Figure 3.2 - Horizontal Section of TAPIRO parallel to the floor.

To allow irradiation experiences, the system has different channels, located in different positions; they are realized with a metallic cylindrical clad and they are filled with plugs made of copper, in the reflector's area, and of shielding material in the external part. The copper part of each plug is removable to permit the insertion of sample material or detectors used for experiences. An important characteristic of the channels is that their sections are gradually reduced to cut down the gamma ray streaming effect. The main channels are shown in Table 3.1) [10]:

<b>Name</b>	<b>Position</b>	<b>Penetration</b>
Diametral channel (D.C.)	Piercing. Horizontal. Diametral in the core.	Inner and outer fixed reflector. Core.
Tangential channel	Piercing. Horizontal. 50 mm above core mid-plane. Parallel to D.C. 106 mm from core axis.	Inner and outer fixed reflector.
Radial channel 1 (R.C.1)	Radial. Horizontal on core mid-plane, at 90° with respect to D.C.	Inner and outer fixed reflector, up to 93 mm from core axis.
Radial channel 2	Radial. Horizontal on core mid-plane, at 50° with respect to R.C.1.	Outer fixed reflector, up to 228 mm from core axis.
Grand Horizontal Channel (G.H.C.)	Radial. Concentric with R.C.1.	Up to reflector outer surface
Grand Vertical Channel (G.V.C.)	Above core, on the same axis.	Outer fixed reflector, up to 100 mm from upper core base.
Thermal column	Horizontal.	Shield, up to outer reflector
Irradiation cavity	On safety plug upper base.	7.4 mm

**Table 3.1 - TAPIRO experimental channels**

## **3.2 TAPIRO MCNP MODEL**

The TAPIRO model implemented in MCNP code is the standard reference model utilized for reactor operation and experiment modelling. It is actually constructed through surface-based cell volumes allowing a complete domain representation of both reactor core, reflector and irradiation channels.

The core is composed of a number of fuel cylindrical plates cooled by helium and a calibration pellet. The central part of the diametral channel is filled by radially oriented pellets as well.

The MCNP results presented here are obtained without the calibration pellet and with the central pellets inserted. In addition, the Safety Rods (SR1 and SR2) and Shim Rods (S1 and S2) are considered inserted.

Considered irradiation channels are the diametrical channel, tangential channel and radial channel 1. They are all filled with air and the copper plugs are also removed.

Nuclear data library utilized is JEFF3-1 provided by NEA Data Bank and processed at 300 K [11].

Model normalization is made at the flux peak according to standard reference [12].

Diametrical channel characterization is obtained through flux evaluation and minor actinides fission and capture reaction rate. This is performed with the mesh tally MCNP feature through which cells are created dividing the actual geometry to obtain the response in a customized calculation grid.

### 3.3 SAMPLING OF CORE FISSION SOURCE

According to usual practice, a decoupled approach has been followed in order to produce a fixed source simulation after an eigenvalue calculation. In fact, scalability - in fixed source simulations - allows better improvement in time efficiency more than eigenvalue simulations.

Foremost, eigenvalue simulations have been carried out in order to prepare the fission source, which has been sampled through the fundamental mode: 20000 cycles were run, made by 10000 histories each.

Source has been sampled by a spatial subdivision of the TAPIRO core, by means of different iterations in an optimization approach.

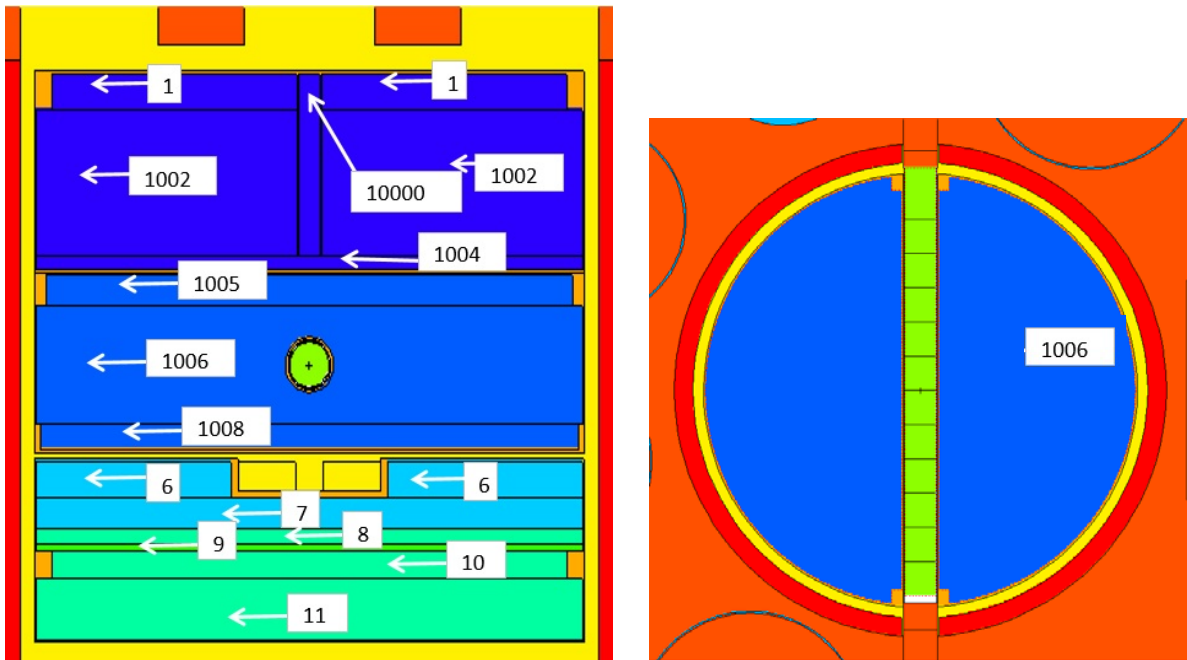


Figure 3.3 - Sections of TAPIRO MCNP input: vertical (left) and horizontal at midcore (right).

The highly enriched cylindrical core has been divided in many horizontal layers (Fig. 3.3 left). In addition, cylindrical shells have been accounted for (Fig. 3.3 right). Thus, the fundamental mode distribution of the flux has been sampled in small volumes through radial and axial binning. Fission production has been tallied in each volume to be used in the following studies as source. Of course each volume averages the fission reaction rate inside itself, introducing an approximation. One could in principle consider a particular fission distribution as source, considering what MCNP stores at the end of each cycle. The latter approach would avoid volume discretization but it would not utilize all the information belonging to all previous cycles.

Initial cell subdivision of the TAPIRO core is depicted in Fig. 3.3, cell numbers are reported as in the standard input which is optimized just for suitable geometrical description of the system.

Considering TAPIRO core as a starting point (Fig. 3.4), division of the fissile portion has been optimized as follows. In principle, azimuthal symmetry seemed to hold at least for radial and diametrical channel responses, which are main part of the analysis to be carried out.

Following steps have been implemented (Fig. 3.5):

- 1) initial geometry is used splitting cells 1002 (in cells 99992, 99993 and 99994) and 1006 (in cells 99995 and 99996) producing the “case 1”
- 2) previous geometry subdivision has been improved introducing more radial bins through the facility available in MCNP by which a response can be tallied according to cell splitting, using several surfaces: “case 2” is then obtained
- 3) more axial bins are introduced in “case 3”, more precisely in central region and relative to initial 1006 cell.
- 4) more radial bins are introduced in “case 4” concerning the outermost portion, since it presents a less regular geometry compared to the approximations of the previous configurations
- 5) particular azimuthal effect is introduced taking into account the diametrical channel which passes through the core. “Case 5” is then prepared using the MCNP facility of rejecting source particles outside a particular cell which is configured as a merge of all fissile portions, reproducing the real TAPIRO core, even inside the diametrical channel which violates the azimuthal symmetry (cookie cutter cell tool).

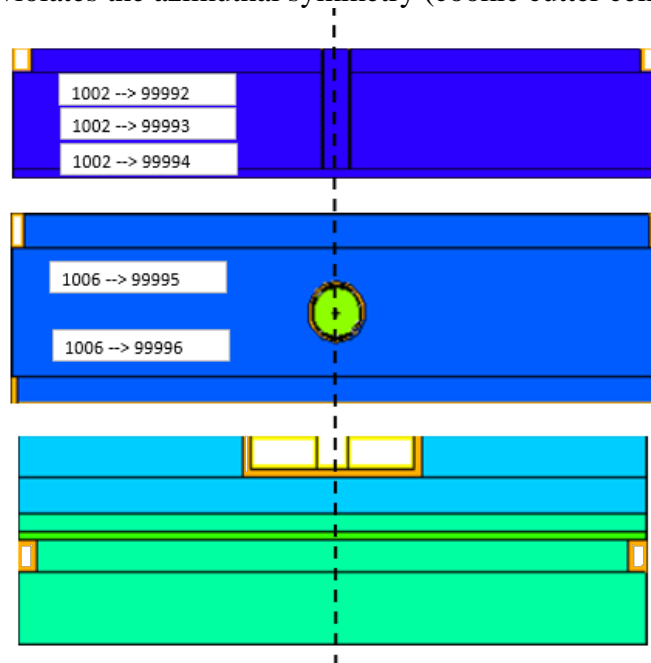


Figure 3.4 - TAPIRO core in MCNP input: vertical split of cylindrical elements.

Each step in the process has been verified in terms of consistency of the sample source to be used in the subsequent simulation – after the decoupling.

Once a fission rate distribution in the volumes is obtained, a fixed source simulation is carried out tallying the same responses in different reactor positions. In particular, neutron

flux in the experimental channels has been considered as a reference for comparisons, values obtained during a previous eigenvalue calculations are considered.

Thus, diametrical, tangential and radial channels basically agreed since the configuration reported at Case 1.

Volumes belonging to diametrical channel inside the core center showed some discrepancy between the eigenvalue results and those obtained through fixed source based on sampled fission distribution.

TAPIRO core is a relatively small and a fast-spectrum nuclear system and this explains how external experimental channels do not require a fine core subdivision, of course central core responses require more precision.

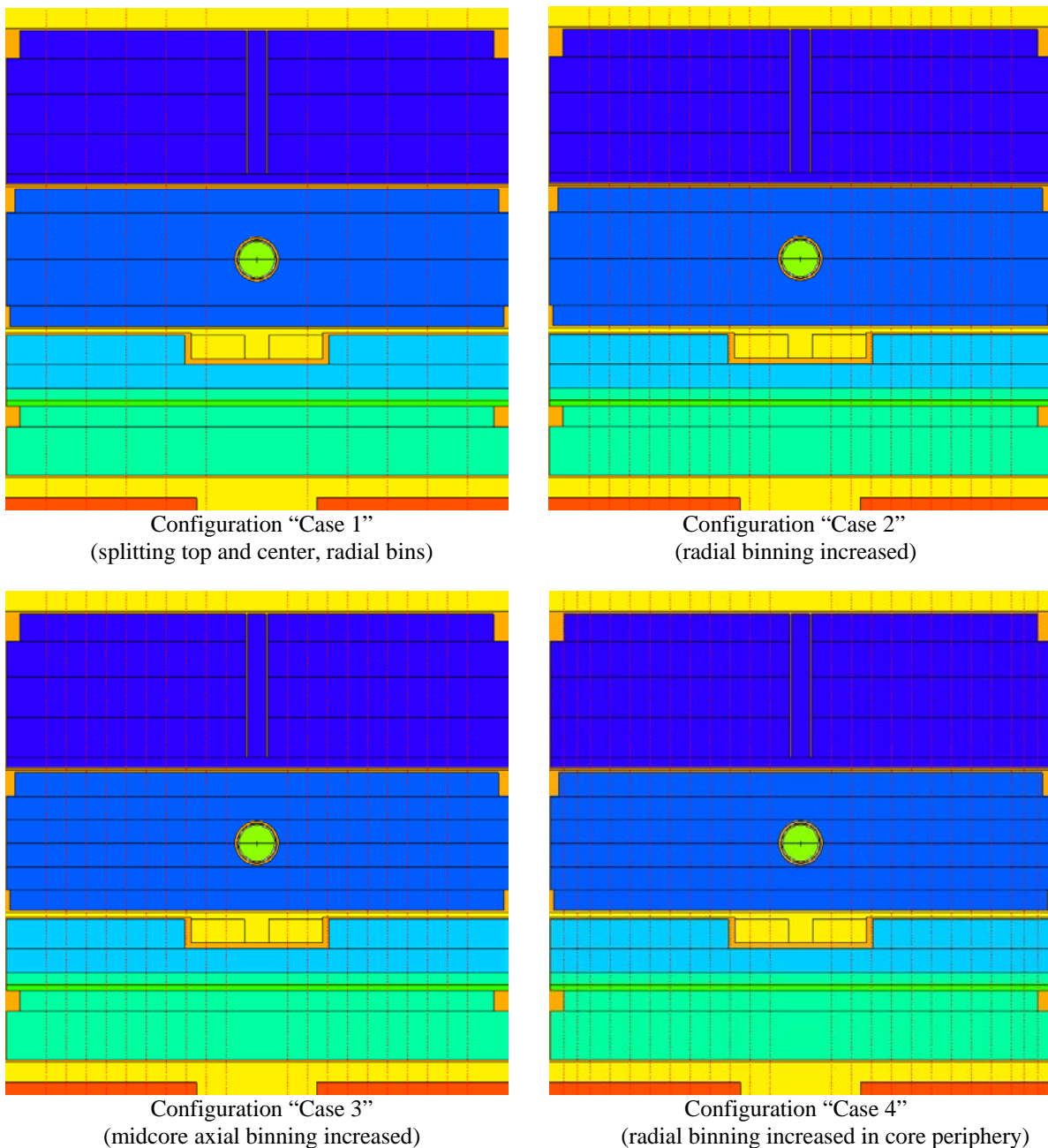


**Figure 3.5 - TAPIRO core in MCNP input: optimization of core splitting for source sampling.**

For each simulation, relative difference between eigenvalue central core flux and those obtained with different core discretization are reported in the plot in Fig. 3.6, with respect to radial coordinate in cm. An acceptable description has been achieved once all differences attained 2% value at most (relative error related to this difference has been calculated as well, being less than 1%).

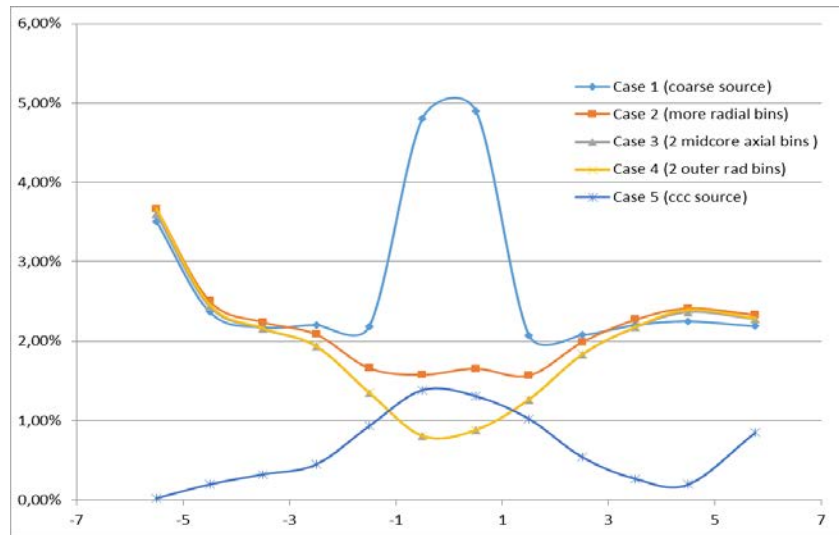


Figure 3.6 - Relative difference between eigenvalue calculation and sampled fixed fission source

Coherence between sampled core source and eigenvalue calculation could have been verified in a number of methods – namely flux leakage from core for instance as in ICRS13 papers cited in the Introduction; the current approach just considered the main objective at which the next simulations are aimed at.

### 3.4 FIXED SOURCE CALCULATIONS

Second stage of present analysis consists of a fixed source simulation, in which the source previously prepared is utilized. This is interesting since different variance reduction techniques are possibly implied in MCNP code: both through source biasing and by means of embedded facilities such as weight window.

In particular, a methodological comparison has been carried out within this study between an analog approach and the Direct Statistical Approach (DSA). Both are utilized and a comparison is outlined.

DSA is an in-house ENEA MCNP patch which optimizes importance values to the calculational domain starting from the evaluation of both second moment and time per history [4-6]. Variance reduction parameters are then obtained minimizing these two functions which contribute to the improvement of the efficiency of the calculation, namely increasing of the Figure of Merit (FOM).

The objective of present simulation is to determine capture and fission reaction rates inside the experimental channels (Fig. 3.7), 11 nuclides are considered for 2 reaction rates each.

In addition, 226 space cells are created to tally reaction rates in the channel as follows:

- diametrical channel (15003 and 15000): 42 + 42 cells
- diametrical channel in core center (55): 12 cells



- tangential channel (44, 42 and 43): 27 + 36 + 27 cells
- radial1 channel (230): 40 cells

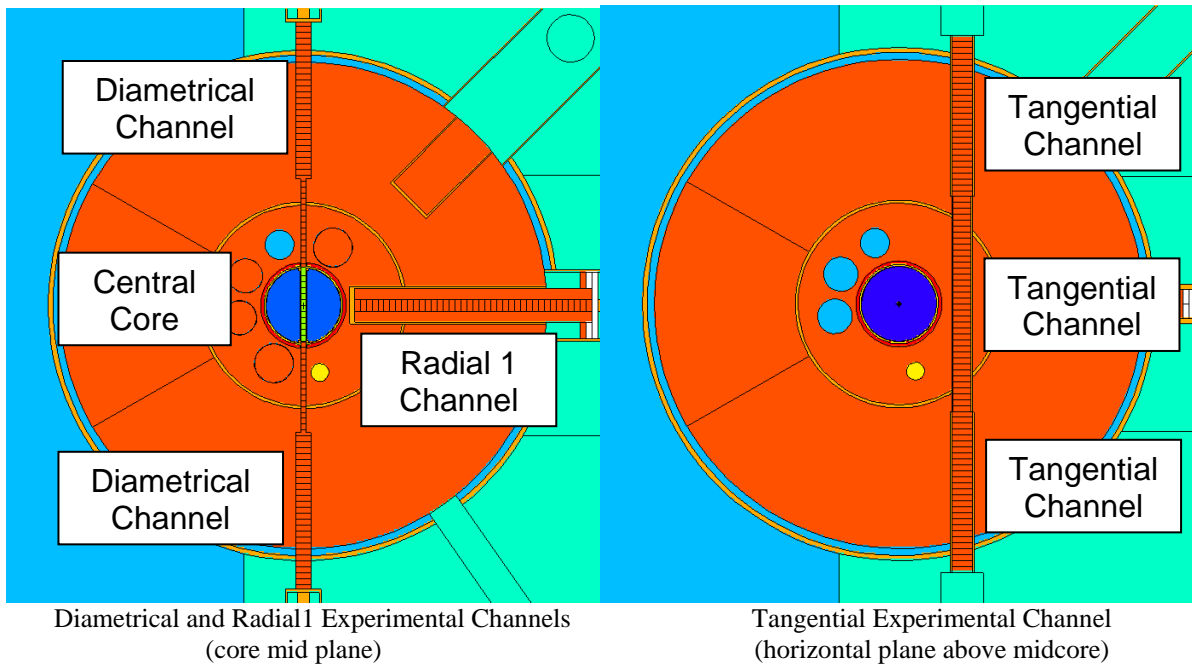


**Figure 3.7 – TAPIRO Experimental channels as in MCNP input description**

Fixed source simulations are performed under two following conditions:

- Analog simulations have been performed with 6 M histories, on cluster system and parallel computing using 24529.16 cpu-min.
- Simulation implementing DSA method for variance reduction improving estimation of the results. 6 M histories are run on cluster system using 29951.00 cpu-min.

### 3.5 EIGENVALUE SIMULATIONS USING DSA

Independent eigenvalue simulations are carried out and DSA methodology for variance reduction is directly implemented at the same time. In fact, multi-response capability is used both for local responses – outside core in experimental channels – and for global responses. Latter global responses are zones in which the core is divided and in these portions the convergence of the fundamental mode is controlled at each superhistory.

This simulation is performed using 60000 cycle, each cycle is made by 10000 histories. Calculation time has been about 64294.83 cpu-min.

### 3.6 RESULTS

Performed simulations were conducted as follows:

- Analog fixed source calculation after source preparation in eigenvalue simulation
- DSA fixed source calculation after source preparation in eigenvalue simulation
- Eigenvalue calculation using DSA variance reduction

Results are showed in the following pictures. Errors are reported in graphical bars. DSA positive effect in methodology and quality of the results is underlined.

### 3.6.1 DIAMETRICAL CHANNEL SIMULATIONS

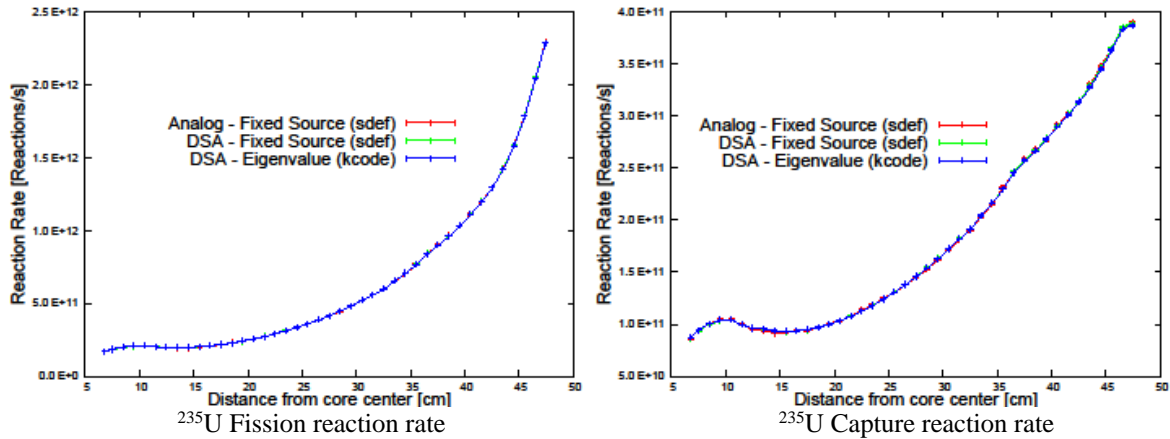


Figure 3.8 – Plots comparing methods for Diametrical Channel:  $^{235}\text{U}$

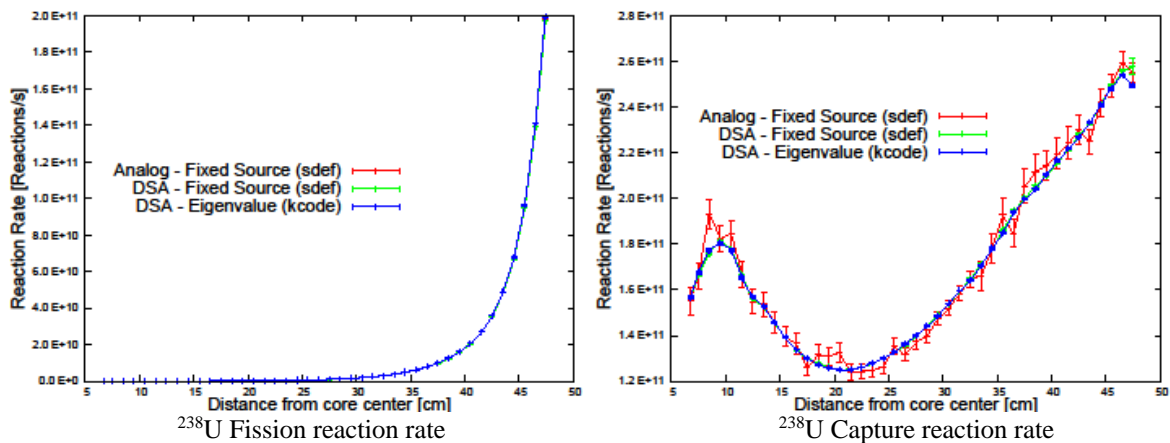


Figure 3.9 – Plots comparing methods for Diametrical Channel:  $^{238}\text{U}$

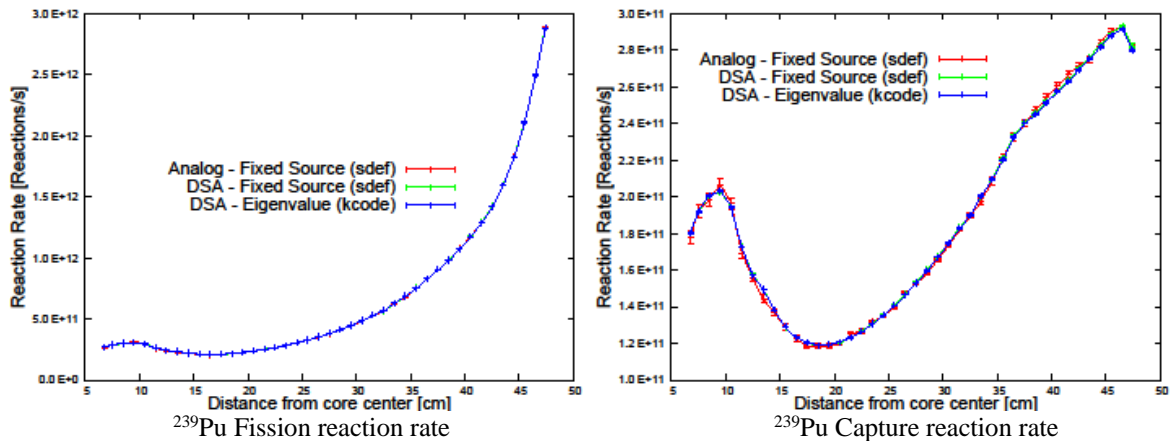


Figure 3.10 – Plots comparing methods for Diametrical Channel:  $^{239}\text{Pu}$

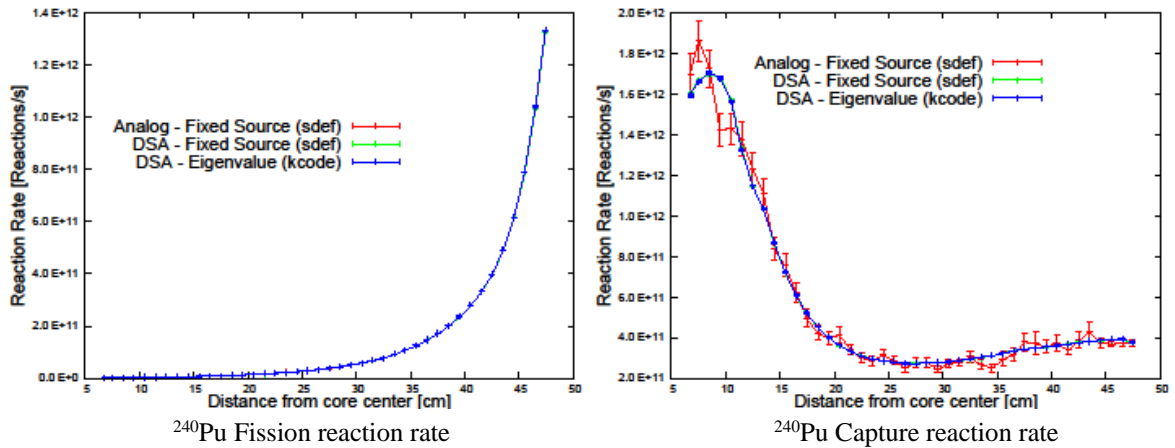


Figure 3.11 – Plots comparing methods for Diametrical Channel:  $^{240}\text{Pu}$

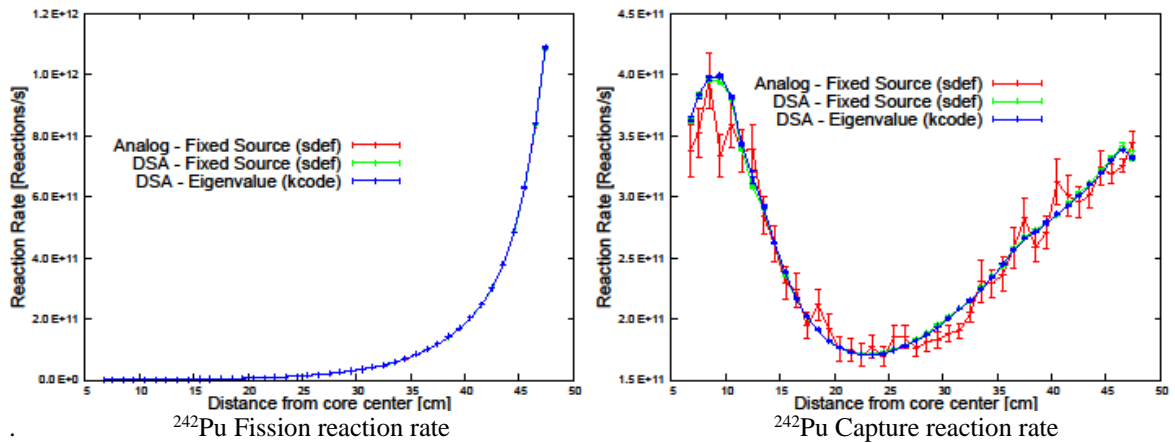


Figure 3.12 – Plots comparing methods for Diametrical Channel:  $^{242}\text{Pu}$

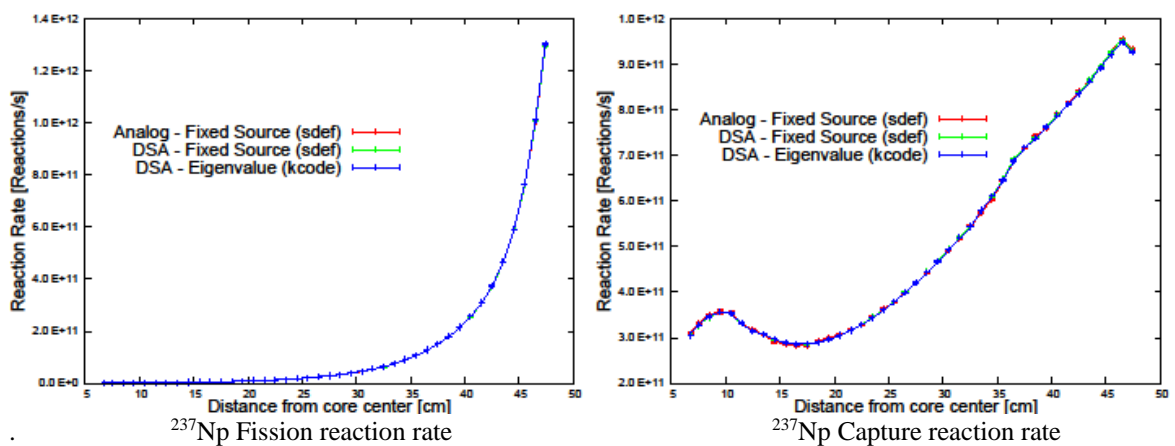


Figure 3.13 – Plots comparing methods for Diametrical Channel:  $^{237}\text{Np}$

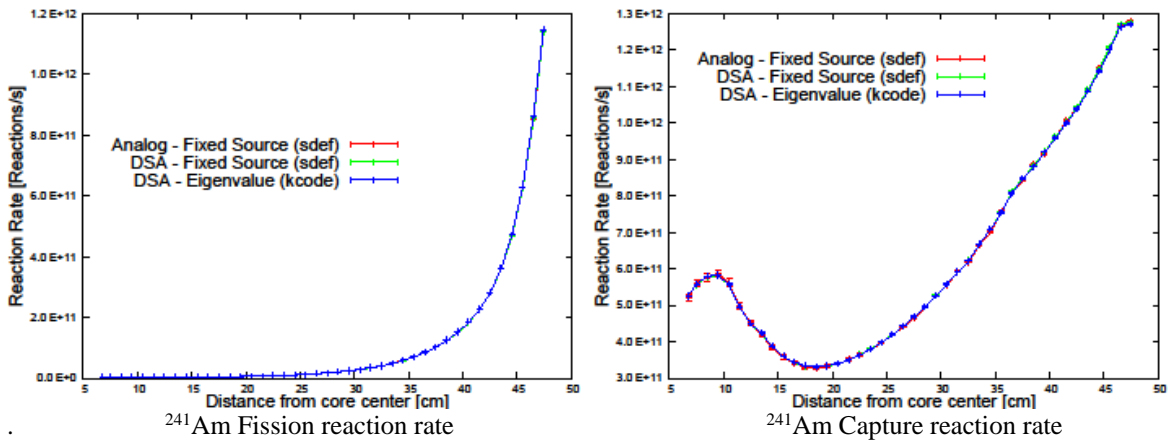


Figure 3.14 – Plots comparing methods for Diametrical Channel:  $^{241}\text{Am}$

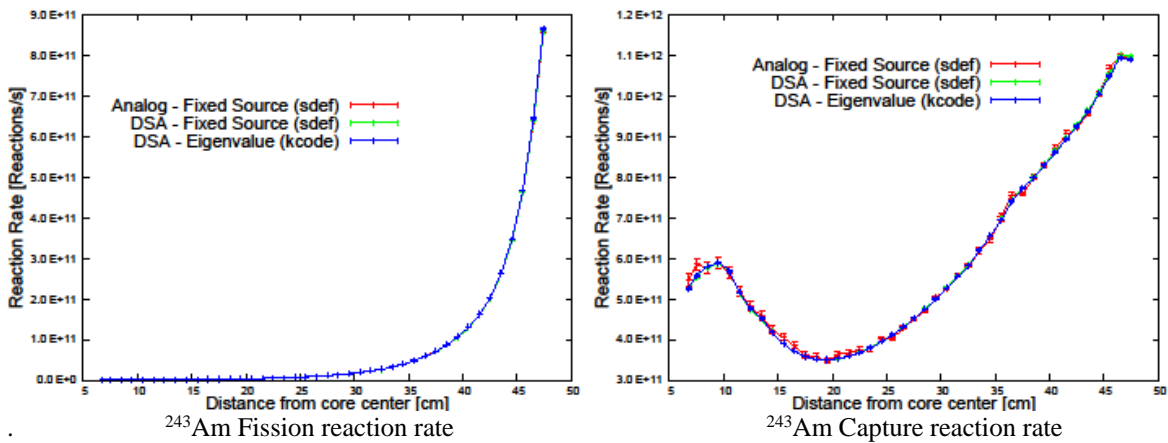


Figure 3.15 – Plots comparing methods for Diametrical Channel:  $^{243}\text{Am}$

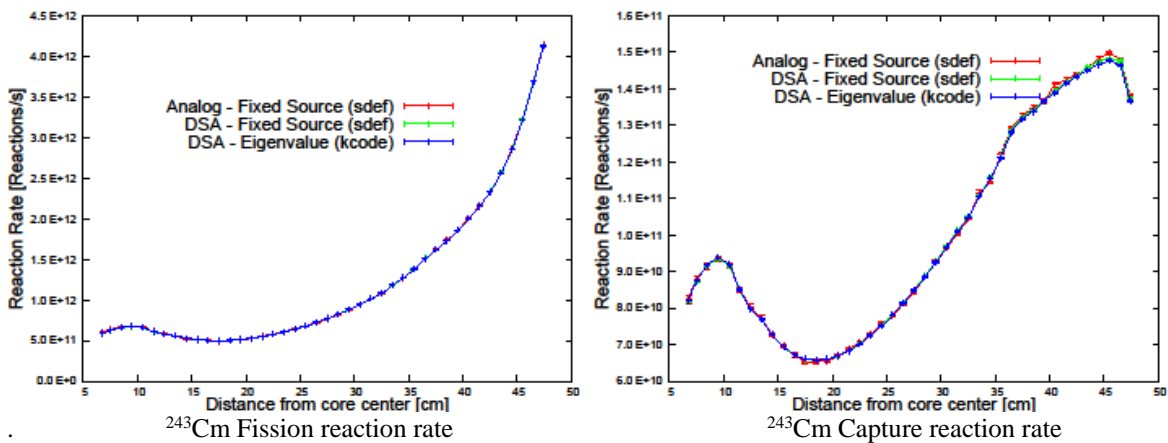


Figure 3.16 – Plots comparing methods for Diametrical Channel:  $^{243}\text{Cm}$

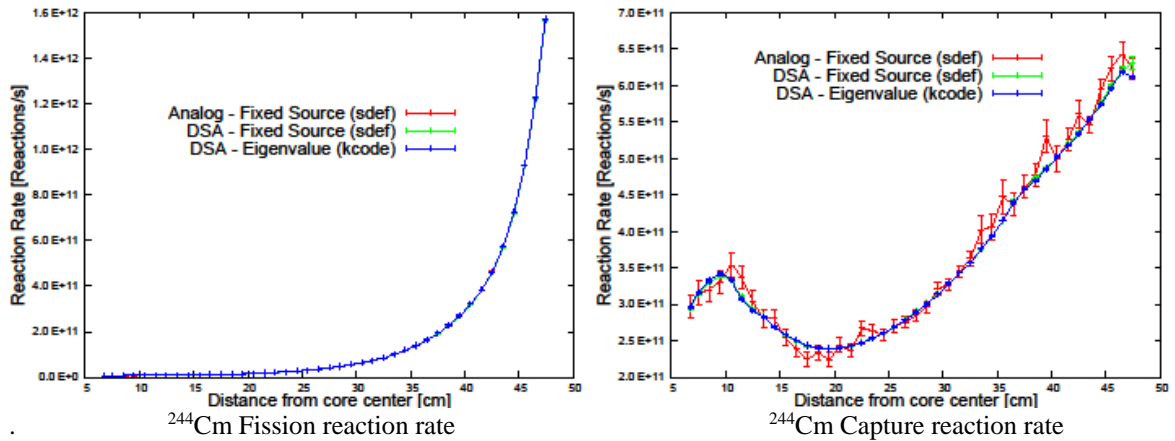


Figure 3.17 – Plots comparing methods for Diametrical Channel: <sup>244</sup>Cm

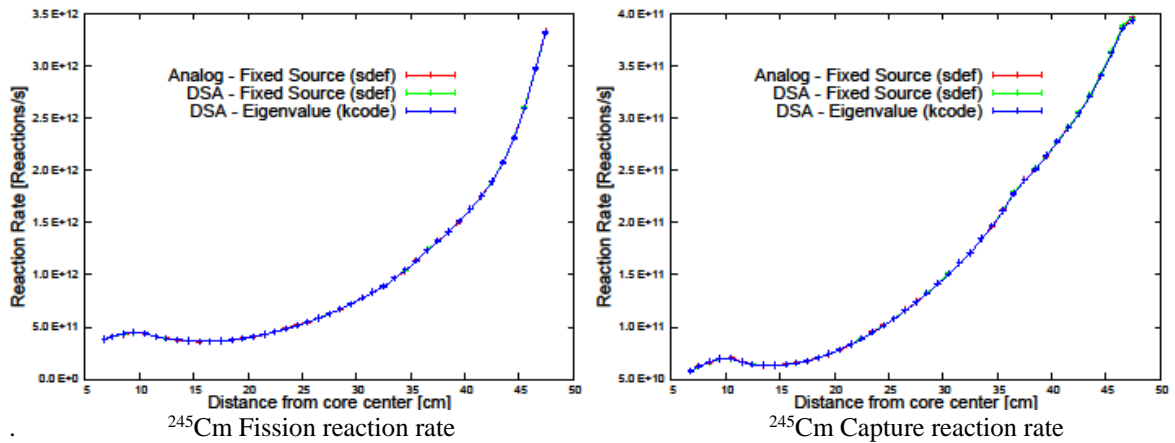


Figure 3.18 – Plots comparing methods for Diametrical Channel: <sup>245</sup>Cm

### 3.6.2 RADIAL 1 CHANNEL SIMULATIONS

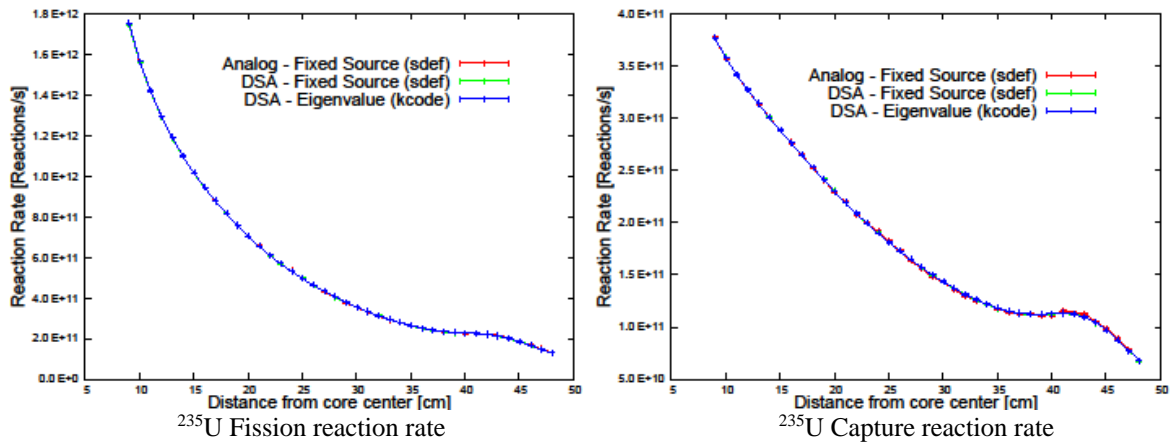


Figure 3.19 – Plots comparing methods for Radial1 Channel:  $^{235}\text{U}$

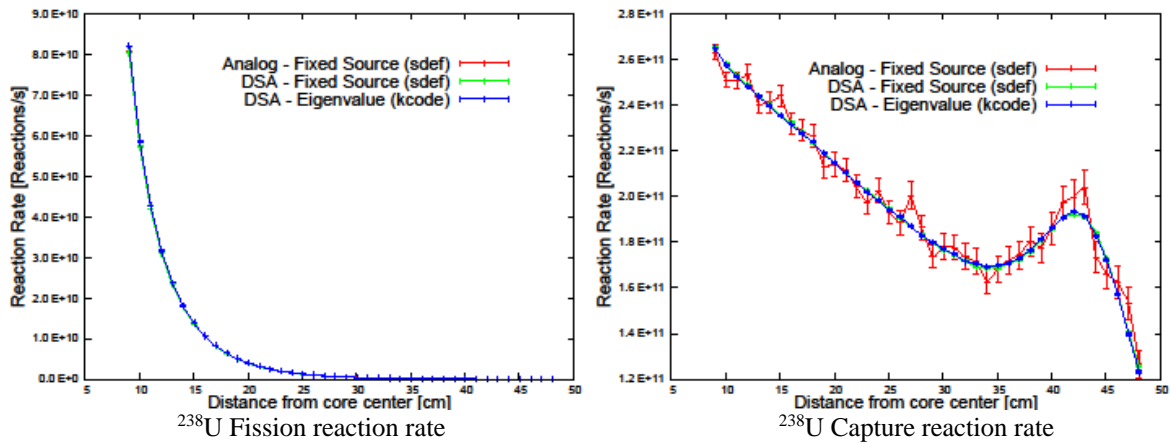


Figure 3.20 – Plots comparing methods for Radial1 Channel:  $^{238}\text{U}$

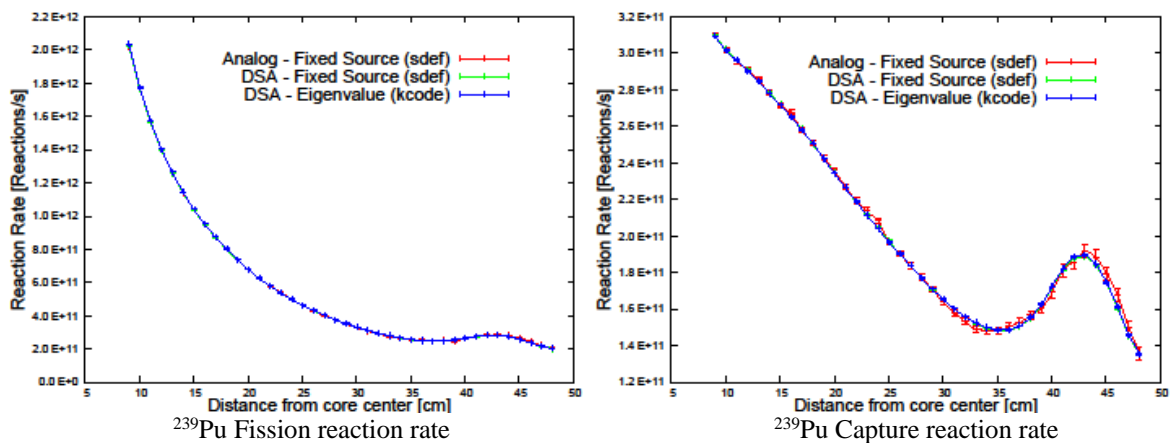


Figure 3.21 – Plots comparing methods for Radial1 Channel:  $^{239}\text{Pu}$

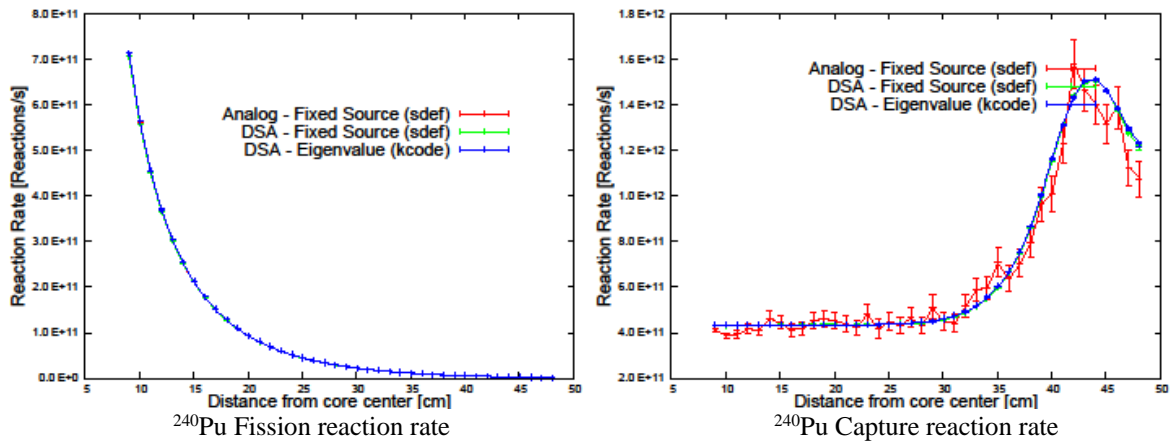


Figure 3.22 – Plots comparing methods for Radial1 Channel:  $^{240}\text{Pu}$

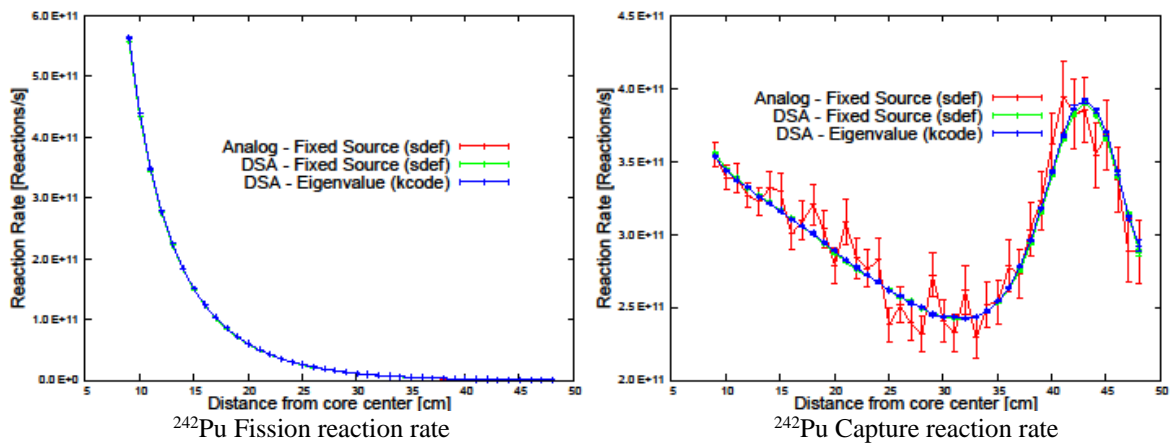


Figure 3.23 – Plots comparing methods for Radial1 Channel:  $^{242}\text{Pu}$

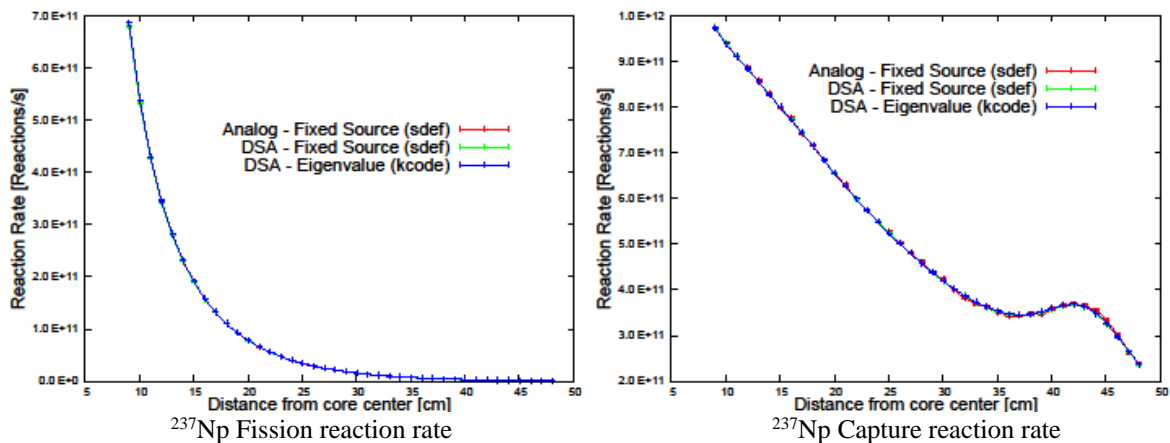


Figure 3.24 – Plots comparing methods for Radial1 Channel:  $^{237}\text{Np}$

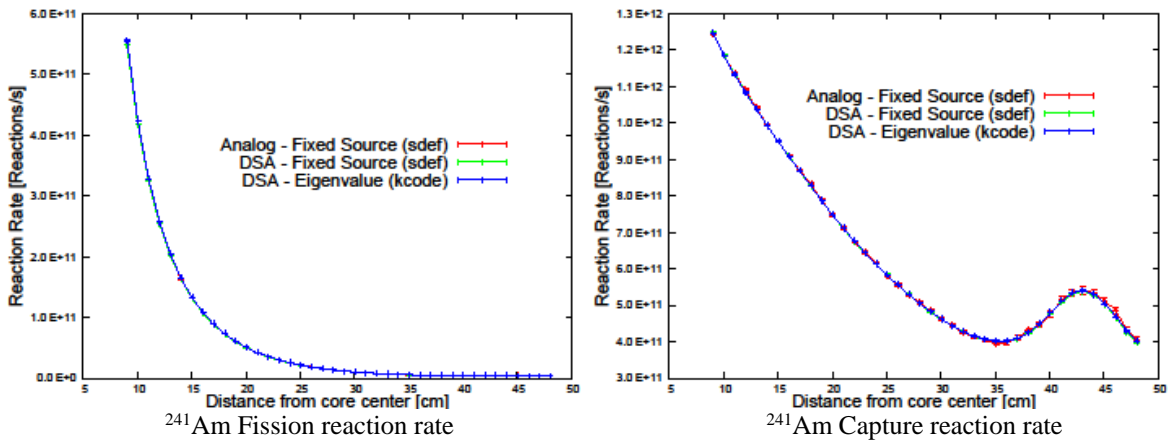


Figure 3.25 – Plots comparing methods for Radial1 Channel:  $^{241}\text{Am}$

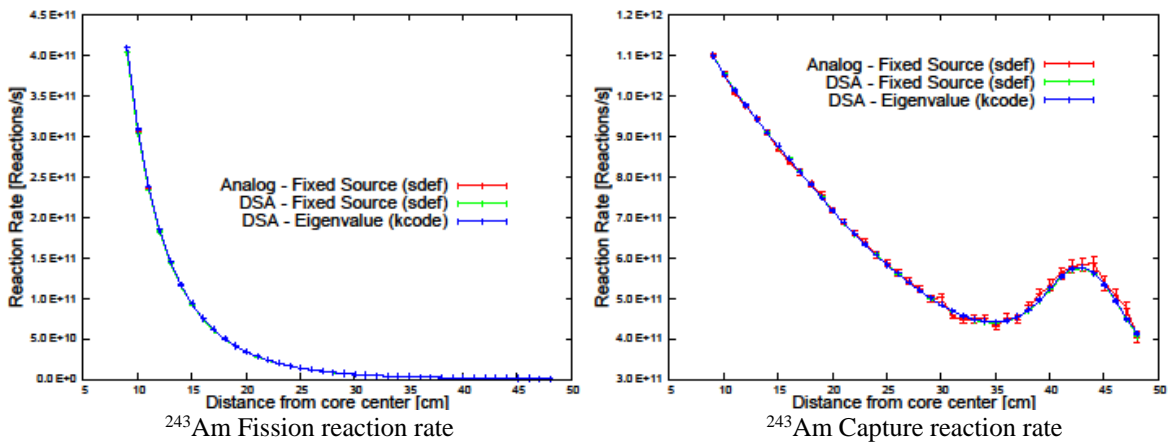


Figure 3.26 – Plots comparing methods for Radial1 Channel:  $^{243}\text{Am}$

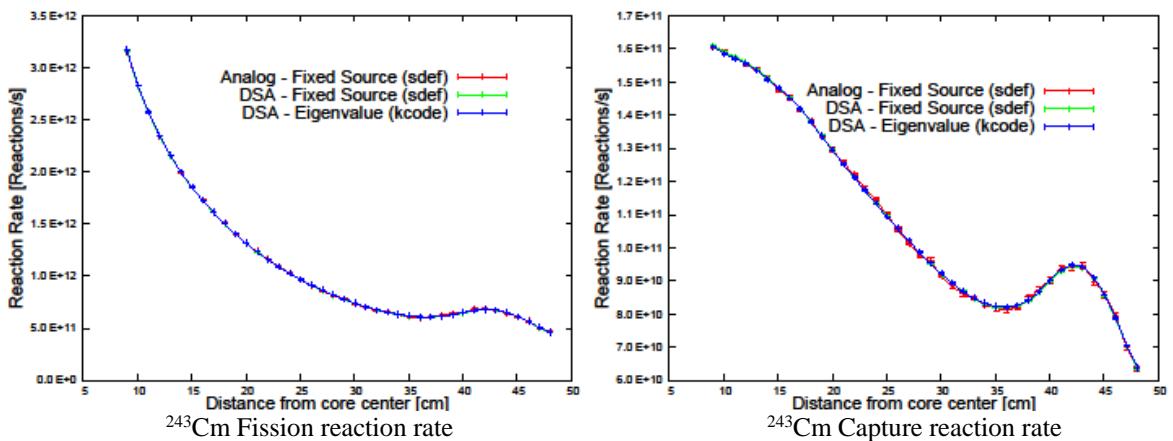


Figure 3.27 – Plots comparing methods for Radial1 Channel:  $^{243}\text{Cm}$



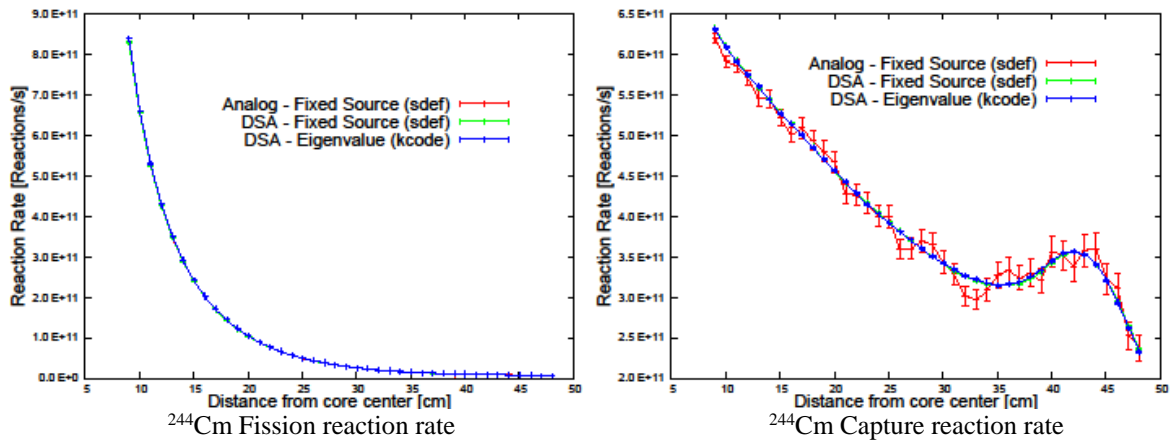


Figure 3.28 – Plots comparing methods for Radial1 Channel: <sup>244</sup>Cm

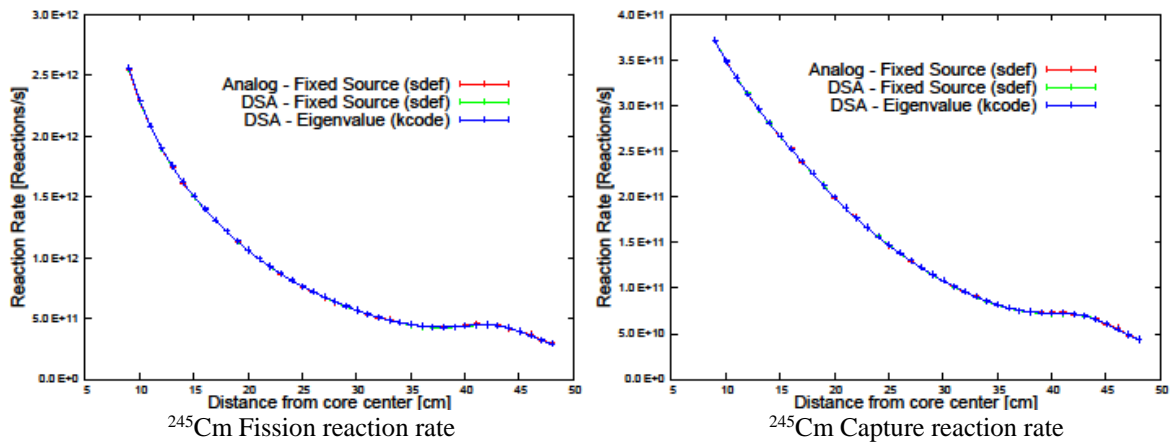


Figure 3.29 – Plots comparing methods for Radial1 Channel: <sup>245</sup>Cm

### 3.6.3 TANGENTIAL CHANNEL SIMULATIONS

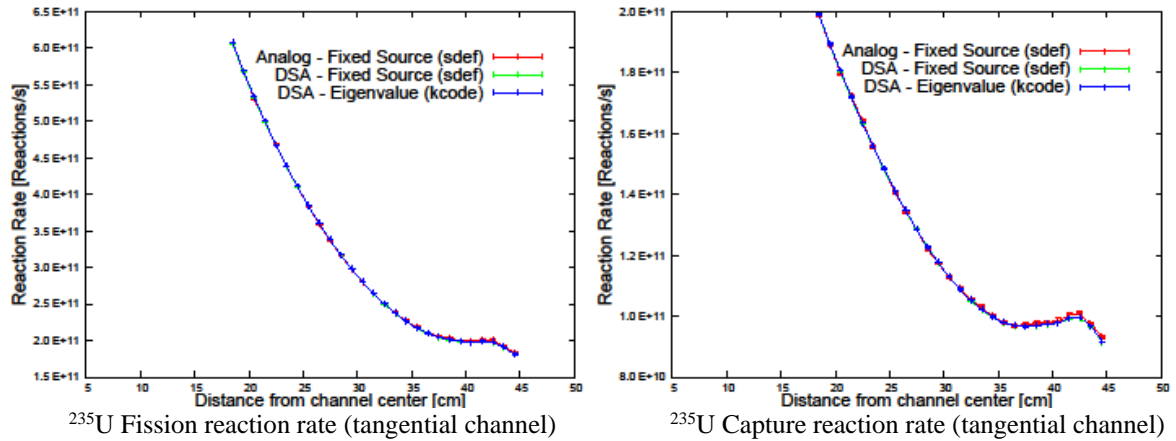


Figure 3.30 – Plots comparing methods for Tangential Channel:  $^{235}\text{U}$

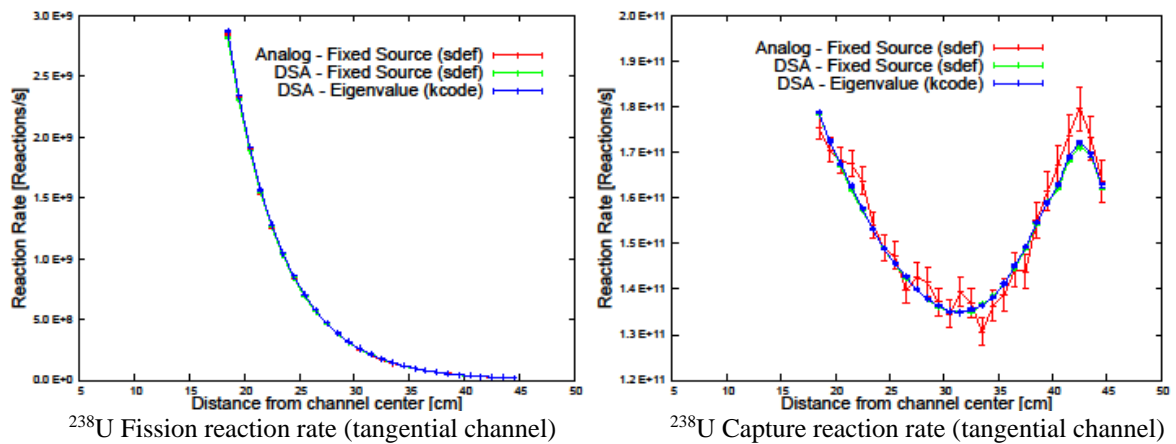


Figure 3.31 – Plots comparing methods for Tangential Channel:  $^{238}\text{U}$

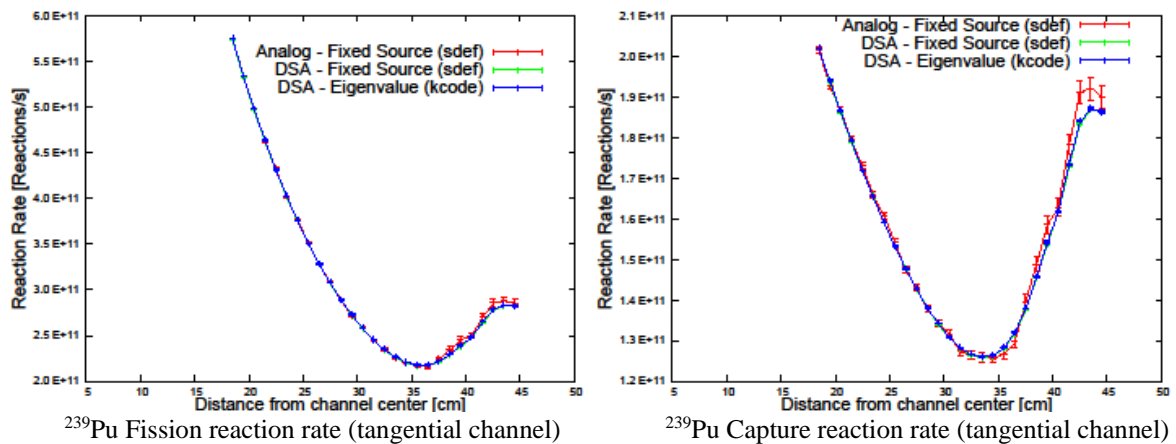


Figure 3.32 – Plots comparing methods for Tangential Channel:  $^{239}\text{Pu}$

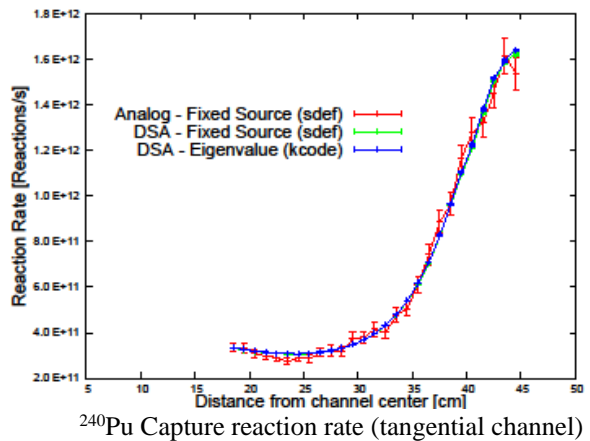
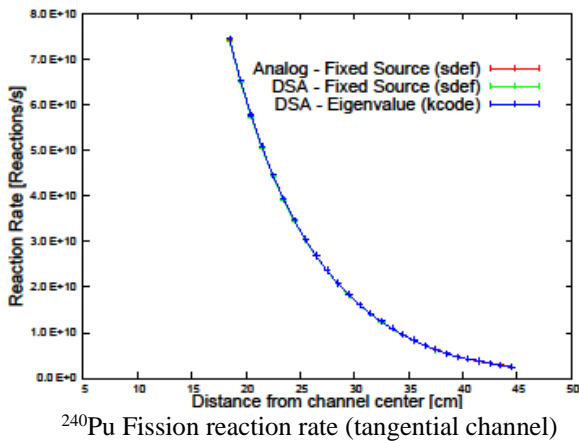


Figure 3.33 – Plots comparing methods for Tangential Channel: <sup>240</sup>Pu

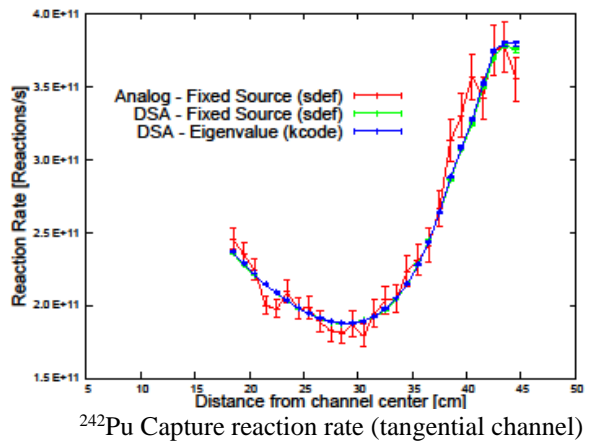
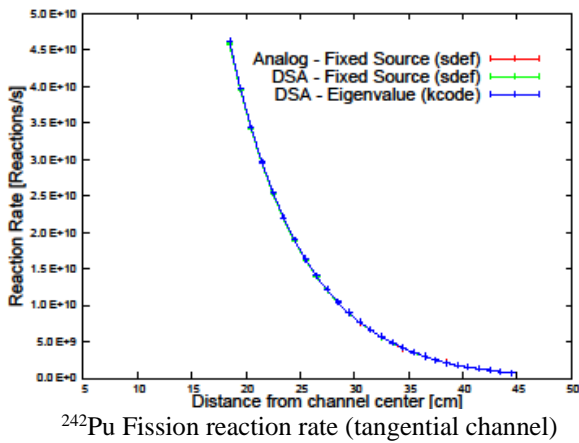


Figure 3.34 – Plots comparing methods for Tangential Channel: <sup>242</sup>Pu

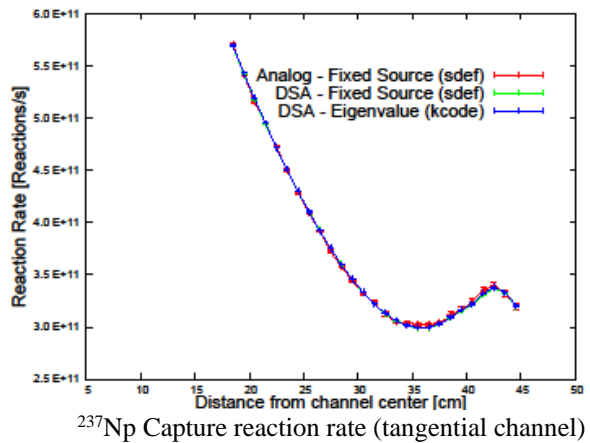
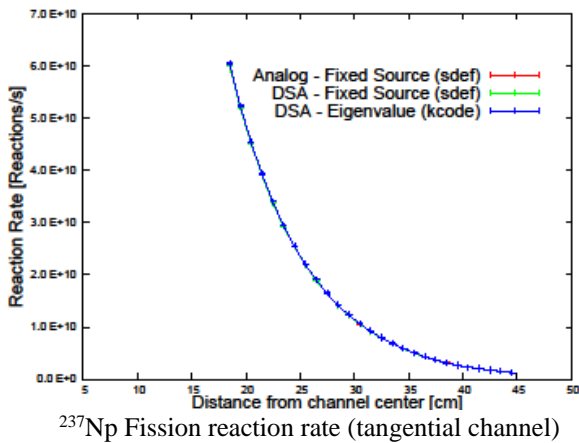
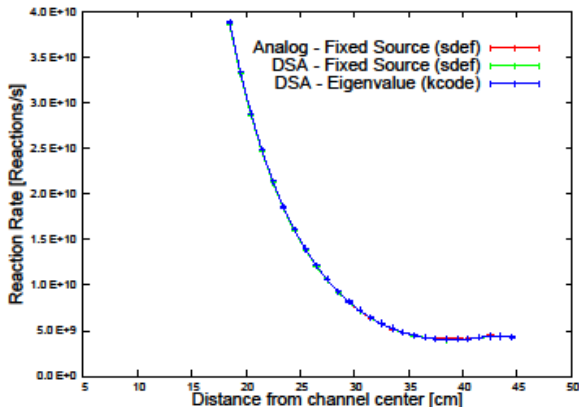
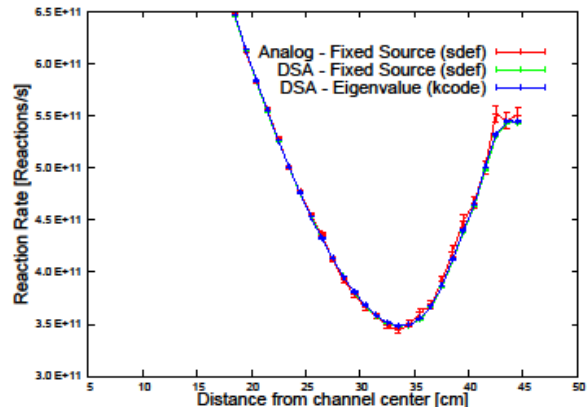


Figure 3.35 – Plots comparing methods for Tangential Channel: <sup>237</sup>Np

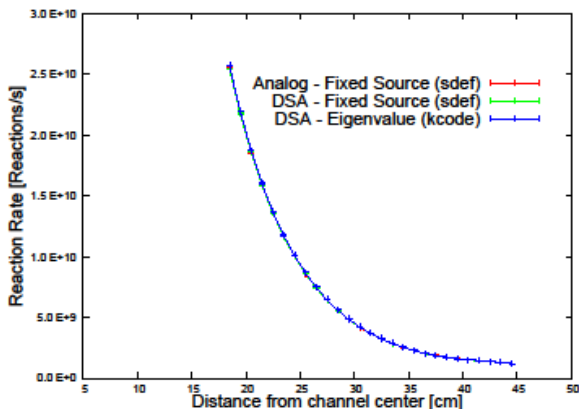


<sup>241</sup>Am Fission reaction rate (tangential channel)

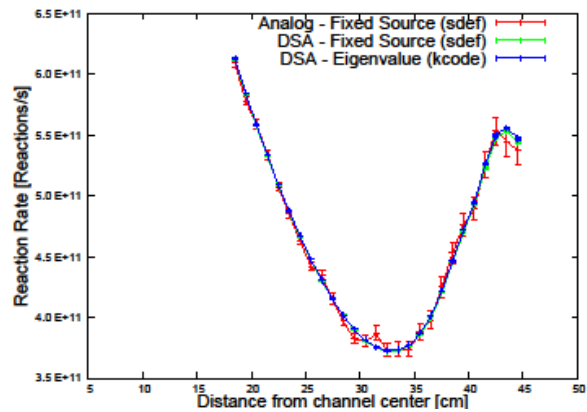


<sup>241</sup>Am Capture reaction rate (tangential channel)

Figure 3.36 – Plots comparing methods for Tangential Channel: <sup>241</sup>Am

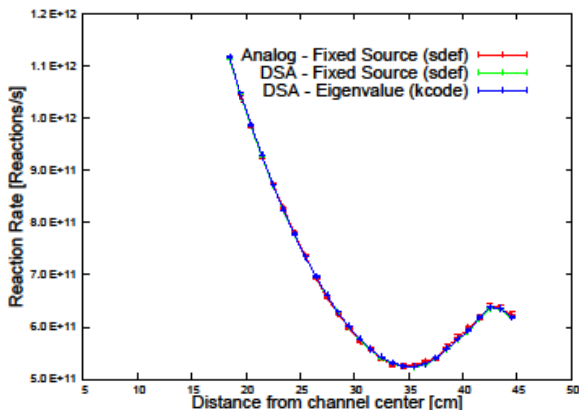


<sup>243</sup>Am Fission reaction rate (tangential channel)

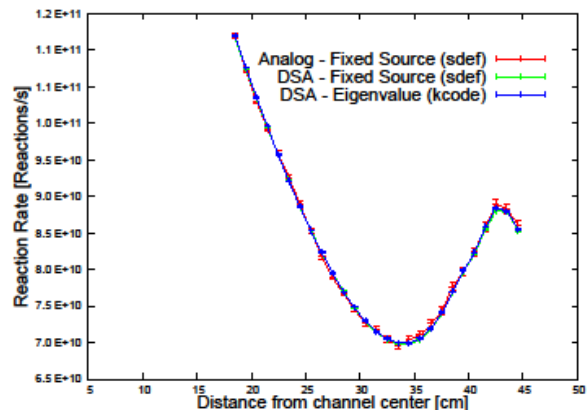


<sup>243</sup>Am Capture reaction rate (tangential channel)

Figure 3.37 – Plots comparing methods for Tangential Channel: <sup>243</sup>Am

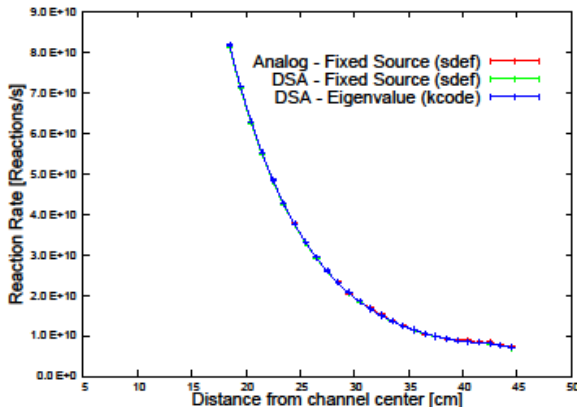


<sup>243</sup>Cm Fission reaction rate (tangential channel)

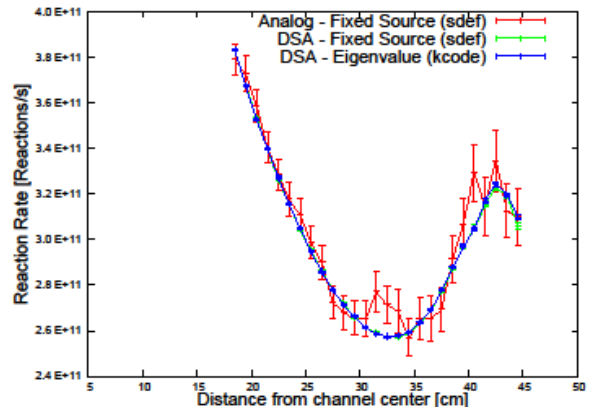


<sup>243</sup>Cm Capture reaction rate (tangential channel)

Figure 3.38 – Plots comparing methods for Tangential Channel: <sup>243</sup>Cm

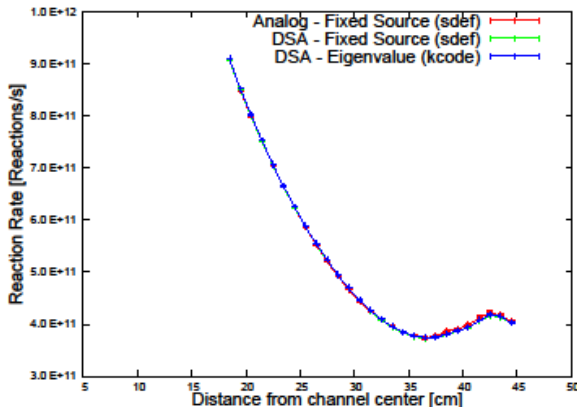


<sup>244</sup>Cm Fission reaction rate (tangential channel)

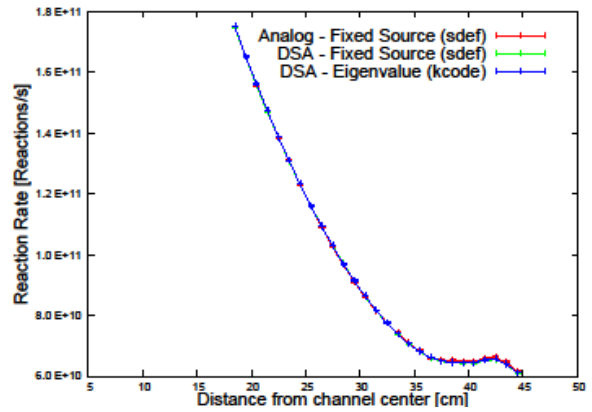


<sup>244</sup>Cm Capture reaction rate (tangential channel)

Figure 3.39 – Plots comparing methods for Tangential Channel: <sup>244</sup>Cm



<sup>245</sup>Cm Fission reaction rate (tangential channel)



<sup>245</sup>Cm Capture reaction rate (tangential channel)

Figure 3.40 – Plots comparing methods for Tangential Channel: <sup>245</sup>Cm

#### 4. PCA-REPLICA BENCHMARK

Within the framework of the TIHANGE simulations implementing DSA methodology, common procedure suggests the verification of the implemented calculational tools with a robust experimental benchmark.

The PCA-Replica low-flux engineering neutron shielding experiment has been considered simple but valuable case for this objective [13-14].

PCA-Replica is a water/iron (H<sub>2</sub>O/Fe) benchmark experiment including two water layers (12cm/13cm) alternated with a PWR thermal shield (TS) simulator and a PWR pressure vessel (RPV) simulator. The PCA-Replica experimental facility (see Fig. 4.1) duplicated exactly the ex-core radial geometry of the ORNL PCA (Pool Critical Assembly) similar experiment (Oak Ridge, US, 1981), simulating the ex-core radial geometry of a PWR. In particular, PCA-Replica reproduced the 12/13 configuration of the PCA experiment with a layer of water of about 12 cm between the core and the thermal shield simulator and a layer of water of about 13 cm between the thermal shield simulator and the pressure vessel simulator. An important feature differentiated the two experiments: the low flux reactor neutron source of the PCA experiment was replaced in the PCA-Replica experiment with a neutron source emitted by a thin fission plate containing highly enriched uranium with a rectangular cross-sectional area identical to that of the PCA reactor source.

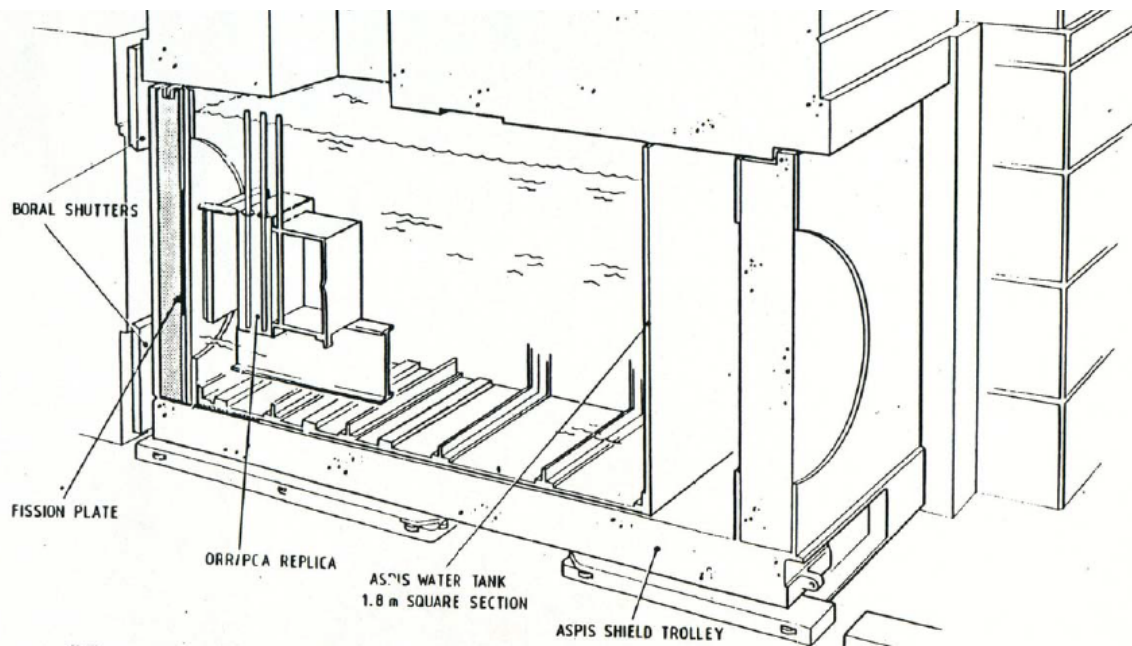


Figure 4.1 – PCA-Replica setup in ASPIS facility at NESTOR research reactor

It is underlined that this simpler source configuration of the PCA-Replica experiment could more easily be calibrated with a high degree of accuracy, reducing in this way a possible cause of the in-vessel neutron flux underpredictions noted in transport analyses dedicated to the PCA experiment, despite the extensive work addressed to obtain an accurate calibration.

## 4.1 GEOMETRY DATA AND MATERIALS

The simple configuration of PCA-Replica and the small source uncertainty make it an interesting case to benchmark calculation methodologies – as it is the case.

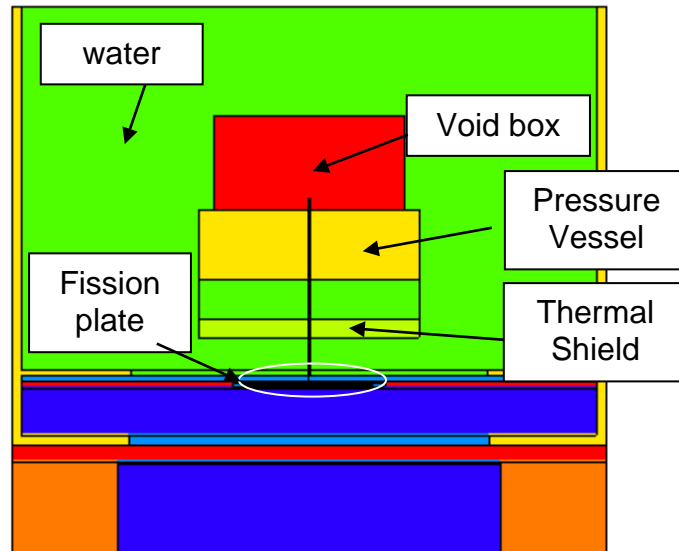


Figure 5.1 – PCA-Replica horizontal section with main materials

The geometry represents the ASPIS facility of the NESTOR reactor. A moving trolley is filled with demineralized water and both a thermal shield sample and a pressure vessel specimen are inserted. The neutron flux gets inside through a particular aluminum window and after moderation by means of a graphite layer.

Fig. 5.1 depicts the main components: the fission plate (source of the problem) is an aluminum uranium alloy AlU (93% enriched in  $^{235}\text{U}$ ) plate with aluminum clad. It is composed by 13 vertical strips, each composed by 4 thin layers.

Thus, produced neutrons cross the aluminum clad and the window up to the water content. The first water layer is 12 cm thick, from the source to the thermal shield plate. Then, 13 cm water layer is between the thermal shield (stainless steel) and the pressure vessel sample (mild steel).

Beyond the pressure vessel specimen, void box is placed to measure leakage current outside the side shield of nuclear reactors. Void box is actually filled with room temperature and pressure air. For material composition, see Table 5.1.

Material	Material Density [g × cm <sup>-3</sup> ]	Element	Weight [%]	Atomic Density [atoms × cm <sup>-3</sup> ]
Graphite	1.65	C	100.0	8.276E+22
Aluminium Cladding	2.70	Al	100.0	6.029E+22
Alloy Fuel (*)	3.257	Al	80.0	5.818E+22
		U-235	18.6	1.552E+21
		U-238	1.4	1.154E+20
Water	1.0	H	11.19	6.688E+22
		O	88.81	3.344E+22
Stainless Steel	7.88	C	0.017	6.721E+19
		Si	0.44	7.438E+20
		Mn	1.57	1.356E+21
		P	0.025	3.832E+19
		S	0.006	8.884E+18
		Cr	18.4	1.688E+22
		Ni	9.4	7.601E+21
		Mo	0.37	1.831E+20
		Ti	0.009	8.920E+18
		Nb	0.014	7.154E+18
		Cu	0.24	1.793E+20
		Fe	69.509	5.909E+22
		Mild Steel	7.835	C
Mn	1.09			9.366E+20
P	0.01			1.524E+19
S	0.032			4.711E+19
Fe	98.648			8.338E+22
Concrete	2.3	Si	33.7	4.120E+22
		Fe	1.4	8.609E+20
		H	1.0	3.407E+22
		O	52.9	1.135E+23
		Al	3.4	4.327E+21
		Ca	4.4	3.770E+21
		Na	1.6	2.390E+21
		K	1.6	1.405E+21

**Table 5.1 - PCA-Replica materials composition**

Neutron cross-sections utilised are JEFF 3.11 processed at 300 K temperature [11]

Benchmark responses are obtained by several detectors counting: <sup>103</sup>Rh103, <sup>115</sup>In and <sup>32</sup>S respectively. Their responses are evaluated within the simulation by means of dosimetric nuclear data as follows: MCNP as-received 531 [15] dos and 532 dos [15], as well as Illos [15] prepared at Lawrence Livermore. In addition, IRDF2002 [16] and IRDFv1.05 [17] are obtained for this simulation and obtained. In fact, 10 dosimeters are place all along the depth of the problem in order to have a good experimantal scannin of the problem even in significant penetration areas (see Fig. 5.2).



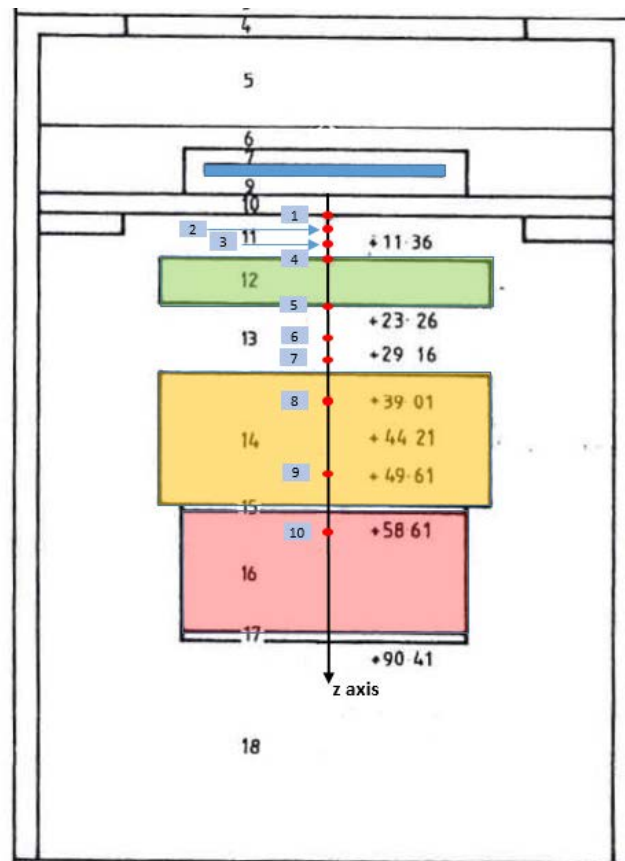


**Figure 5.2 – PCA-Replica setup: 10 detectors positioned at different depths: fission plate (blue) thermal shield (green), vessel (yellow) and void box (red)**

Simulations are performed both in analog mode and implementing variance reduction DSA methodology. Results are reported in following tables. Experimental values are compared with MCNP simulations results corrected for the background due to NESTOR core leakage: it yields 2% flux increase in all positions except for positions 8,9 and 10 in which it yields 4% flux increase. Dosimeters rely on different nuclear reaction thresholds: 0.69 MeV for  $^{103}\text{Rh}$ , 1.30 MeV for  $^{115}\text{In}$  and 2.7 MeV for  $^{32}\text{S}$ . Thus, this simulation appears to be a significant penetration problem concerning phase space in position and energy.

Results for analog simulations are reported as follows:

- $^{103}\text{Rh}$  detectors in positions 1 to 10 (systematic error about 3.00% in all positions, statistical error 3.00% in positions 1-5, 4.00% in positions 6 and 7, 1.00% in position 8, 1.90% in position 9 and 1.60% in position 10).
- $^{115}\text{In}$  detectors in positions 8-10 (systematic error about 2.00% and 0.90% in 8, 1.40% in 9 and 1.50% in 10).
- $^{32}\text{S}$  detectors are placed in position 8-10 as well (systematic error about 4.00% in all positions, 1.50% in position 8, 1.90% in position 9 and 1.30% in position 10).

	Nuclear Data	Value	MCNP Error	Correction	Experimental	C/E
<b>Position 1</b> z = 1.91 cm	LLDOS	1.72703E-20	0.05%	1.76157E-20		<b>1.04</b>
	IRDF2002	1.71871E-20	0.05%	1.75308E-20	<b>1.69E-20</b>	<b>1.04</b>
	IRDFv1.05	1.71871E-20	0.05%	1.75308E-20		<b>1.04</b>
<b>Position 2</b> z = 7.41 cm	LLDOS	3.50172E-21	0.10%	3.57175E-21		<b>0.94</b>
	IRDF2002	3.48618E-21	0.10%	3.55590E-21	<b>3.78E-21</b>	<b>0.94</b>
	IRDFv1.05	3.48618E-21	0.10%	3.55590E-21		<b>0.94</b>
<b>Position 3</b> z = 12.41 cm	LLDOS	1.28605E-21	0.17%	1.31177E-21		<b>0.94</b>
	IRDF2002	1.28154E-21	0.17%	1.30717E-21	<b>1.40E-21</b>	<b>0.93</b>
	IRDFv1.05	1.28154E-21	0.17%	1.30717E-21		<b>0.93</b>
<b>Position 4</b> z = 14.01 cm	LLDOS	1.11598E-21	0.18%	1.13830E-21		<b>0.90</b>
	IRDF2002	1.11136E-21	0.18%	1.13359E-21	<b>1.27E-21</b>	<b>0.89</b>
	IRDFv1.05	1.11136E-21	0.18%	1.13359E-21		<b>0.89</b>
<b>Position 5</b> z = 19.91 cm	LLDOS	4.21814E-22	0.28%	4.30250E-22		<b>1.02</b>
	IRDF2002	4.18868E-22	0.29%	4.27245E-22	<b>4.23E-22</b>	<b>1.01</b>
	IRDFv1.05	4.18868E-22	0.29%	4.27245E-22		<b>1.01</b>

	Nuclear Data	Value	MCNP Error	Correction	Experimental	C/E
<b>Position 6</b> z = 25.41 cm	LLDOS	1.06927E-22	0.49%	1.09066E-22		<b>0.95</b>
	IRDF2002	1.06602E-22	0.49%	1.08734E-22	<b>1.15E-22</b>	<b>0.95</b>
	IRDFv1.05	1.06602E-22	0.49%	1.08734E-22		<b>0.95</b>
<b>Position 7</b> z = 30.41 cm	LLDOS	4.34483E-23	0.77%	4.43173E-23		<b>0.94</b>
	IRDF2002	4.33903E-23	0.78%	4.42581E-23	<b>4.73E-23</b>	<b>0.94</b>
	IRDFv1.05	4.33903E-23	0.78%	4.42581E-23		<b>0.94</b>
<b>Position 8</b> z = 39.01 cm	LLDOS	2.04225E-23	1.00%	2.12394E-23		<b>1.03</b>
	IRDF2002	2.01942E-23	1.02%	2.10020E-23	<b>2.07E-23</b>	<b>1.01</b>
	IRDFv1.05	2.01942E-23	1.02%	2.10020E-23		<b>1.01</b>
<b>Position 9</b> z = 49.61 cm	LLDOS	5.88046E-24	1.69%	6.11567E-24		<b>1.11</b>
	IRDF2002	5.72351E-24	1.74%	5.95245E-24	<b>5.53E-24</b>	<b>1.08</b>
	IRDFv1.05	5.72351E-24	1.74%	5.95245E-24		<b>1.08</b>
<b>Position 10</b> z = 58.61 cm	LLDOS	1.69766E-24	2.86%	1.76556E-24		<b>0.98</b>
	IRDF2002	1.64583E-24	2.95%	1.71166E-24	<b>1.80E-24</b>	<b>0.95</b>
	IRDFv1.05	1.64583E-24	2.95%	1.71166E-24		<b>0.95</b>

Table 5.2 - PCA-Replica results for <sup>103</sup>Rh detectors in all 10 positions


	Nuclear Data	Value	MCNP Error	Correction	Experimental	C/E
<b>Position 8</b> z = 39.01 cm	531DOS	3.73688E-24	1.39%	3.88635E-24		<b>0.99</b>
	532DOS	3.73688E-24	1.39%	3.88635E-24	<b>3.93E-24</b>	<b>0.99</b>
	IRDF2002	3.94544E-24	1.38%	4.10326E-24		<b>1.04</b>
	IRDFv1.05	3.92354E-24	1.37%	4.08049E-24		<b>1.04</b>
<b>Position 9</b> z = 49.61 cm	531DOS	7.92867E-25	2.85%	8.24582E-25		<b>1.00</b>
	532DOS	7.92867E-25	2.85%	8.24582E-25	<b>8.23E-25</b>	<b>1.00</b>
	IRDF2002	8.44322E-25	2.82%	8.78095E-25		<b>1.07</b>
	IRDFv1.05	8.40239E-25	2.81%	8.73848E-25		<b>1.06</b>
<b>Position 10</b> z = 58.61 cm	531DOS	2.06125E-25	5.04%	2.14370E-25		<b>0.93</b>
	532DOS	2.06125E-25	5.04%	2.14370E-25	<b>2.31E-25</b>	<b>0.93</b>
	IRDF2002	2.20132E-25	4.95%	2.28937E-25		<b>0.99</b>
	IRDFv1.05	2.19314E-25	4.93%	2.28086E-25		<b>0.99</b>

Table 5.3 - PCA-Replica results for <sup>115</sup>In detectors in positions 8-9-10

	Nuclear Data	Value	MCNP Error	Correction	Experimental	C/E
<b>Position 8</b> <b>z = 39.01 cm</b>	<b>531DOS</b>	1.05130E-24	2.52%	1.09335E-24		<b>1.01</b>
	<b>532DOS</b>	9.65787E-25	2.55%	1.00442E-24	<b>1.08E-24</b>	<b>0.93</b>
	<b>LLDOS</b>	9.65787E-25	2.55%	1.00442E-24		<b>0.93</b>
	<b>IRDF2002</b>	9.59899E-25	2.56%	9.98295E-24		<b>0.92</b>
	<b>IRDFv1.05</b>	1.03108E-24	2.49%	1.07233E-24		<b>0.99</b>
<b>Position 9</b> <b>z = 49.61 cm</b>	<b>531DOS</b>	1.67835E-25	6.14%	1.74548E-25		<b>1.20</b>
	<b>532DOS</b>	1.54150E-25	6.27%	1.60316E-25	<b>1.46E-25</b>	<b>1.10</b>
	<b>LLDOS</b>	1.54150E-25	6.27%	1.60316E-25		<b>1.10</b>
	<b>IRDF2002</b>	1.52728E-25	6.26%	1.58837E-25		<b>1.09</b>
	<b>IRDFv1.05</b>	1.65766E-25	6.07%	1.72397E-25		<b>1.18</b>
<b>Position 10</b> <b>z = 58.61 cm</b>	<b>531DOS</b>	3.97266E-26	11.70%	4.13157E-26		<b>1.11</b>
	<b>532DOS</b>	3.68432E-26	12.17%	3.83169E-26	<b>3.73E-26</b>	<b>1.03</b>
	<b>LLDOS</b>	3.68435E-26	12.17%	3.83172E-26		<b>1.03</b>
	<b>IRDF2002</b>	3.60467E-26	11.98%	3.74885E-26		<b>1.01</b>
	<b>IRDFv1.05</b>	3.91661E-26	11.55%	4.07327E-26		<b>1.09</b>

**Table 5.4 - PCA-Replica results for <sup>32</sup>S detectors in positions 8-9-10**

PCA-Replica activity is still ongoing and the final objective is to provide simulations in support of the Tihange simulations verifying firstly reliability of nuclear data. DSA is currently implemented to reduce error in results, mainly in positions far from the fission plate and concerning detectors with high energy threshold.

 <b>Ricerca Sistema Elettrico</b>	<b>Sigla di identificazione</b>	<b>Rev.</b>	<b>Distrib.</b>	<b>Pag.</b>	<b>di</b>
	<b>ADPFISS-LP1-079</b>	0	L	34	45


### *Acknowledgements*

Mariya Brovchenko (IRSN, Fontenay-aux-Roses, France) supplied the TIHANGE MCNP model and the simplified generic PWR GEN-III model for calculation comparison and defined the ex-core responses of interest.

Mario Carta and Georgios Glinatsis (ENEA, Casaccia, Italy) conceived the actinide measurement proposal and Valentina Fabrizio and Alfonso Santagata (ENEA, Casaccia, Italy) supplied the TAPIRO geometry model.

### References:

1. MCNP Team, LA-UR-05-8617 (2005)
2. J.T. Goorley *et al.*, LA-UR-13-22934 (2013)
3. K.W. Burn, Nucl. Technol. **175-1** 138-145 (2011)
4. K.W. Burn, Ann. Nucl. Energy, **73**, 218 (2014)
5. K.W. Burn, Ann. Nucl. Energy, **85**, 776 (2015)
6. K.W. Burn, *PHYSOR 2014*, JAERI-Conf 2014-003 (2014)
7. G. Ponti *et al.*, Proc. of the 2014 International Conference on High Performance Computing and Simulation, HPCS 2014, 1030
8. L.Tillard, « Validation des calculs d'irradiation ex-core dans un réacteur à eau sous pression en comparant plusieurs méthodes de réduction de variance », IRSN PSN-EXP/SNC/2016-338
9. Expert Group on Improvement of Integral Experiments Data for minor Actinide Management (EIGEMAM-II), Nuclear Energy Agency (NEA), <https://www.oecd-nea.org/science/ma-ii/>
10. ENEA: General Information and Technical Data of TAPIRO Research Reactor <http://www.enea.it/en/research-development/documents/nuclear-fission/tapiro-eng-pdf>
11. Nuclear Energy Agency – Nuclear Data Bank: Joint European Fission and Fusion library: [http://www.oecd-nea.org/dbforms/data/eva/evatapes/jeff\\_31/](http://www.oecd-nea.org/dbforms/data/eva/evatapes/jeff_31/)
12. M. Carta, M. Palomba, "TRIGA RC-1 and TAPIRO, ENEA Research Reactors", ENEA, Italian National Agency for New Technologies, Energy and Sustainable Economic Development C.R Casaccia, Wien, June 10-12, 2013.
13. J. Butler, M.D. Carter, I.J. Curl, M.R. March, A.K. McCracken, M.F. Murphy, A. Packwood, The PCA-Replica Experiment Part I Winfrith Measurements and Calculations, UKAEA, AEE Winfrith Report AEEW-R 1736, January 1984
14. J. Butler, The NESTOR Shielding and Dosimetry Improvement Programme NESDIP for PWR Applications, PRPWG/P (82)5, Internal UKAEA Document, November 1982.
15. R. C. Little and R. E. Seamon, Dosimetry/Activation Cross Sections for MCNP, MS B226, LANL Memorandum
16. International Reactor Dosimetry File IRDF-2002, IAEA website <https://www-nds.iaea.org/irdf2002/index.htmlx>
17. International Reactor Dosimetry and Fusion File, IRDFF v.1.05 <https://www-nds.iaea.org/IRDFF/>

 <b>Ricerca Sistema Elettrico</b>	Sigla di identificazione	Rev.	Distrib.	Pag.	di
	<b>ADPFISS-LP1-079</b>	0	L	35	45

## APPENDIX: COMPARISON OF DECOUPLED AND SINGLE CALCULATIONAL APPROACH FOR TWO COMPLEMENTARY SAMPLE PROBLEMS




**Radiation transport out from the reactor core: to decouple or not to decouple**

Kenneth W. Burn, Patrizio Console Camprini  
 ENEA  
 Bologna, Italy

1

Radiation transport out from the reactor core: to decouple or not to decouple



1: Background


2: Problem statement

3: Methodology

4: Sample Problems

5: Conclusions



 <b>Ricerca Sistema Elettrico</b>	<b>Sigla di identificazione</b>	<b>Rev.</b>	<b>Distrib.</b>	<b>Pag.</b>	<b>di</b>
	<b>ADPFISS-LP1-079</b>	0	L	36	45

Out from the core: to decouple or not to decouple

1: Background



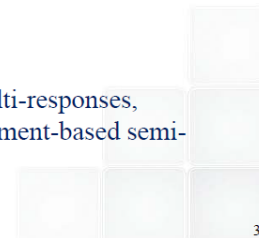
## 1: Background

We have been working for many years on semi-automatic methods to optimize variance reduction parameters in fixed source Monte Carlo radiation transport.

Such methods are based on 3 basic axioms:

- 1) A general variance reduction technique that may be applied to any particle, *viz.* splitting and Russian roulette at phase space surfaces independent of, or dependent on, the weight of the progenitor (to fit, if necessary, with any biasing that may also be present).
- 2) Employment only of Monte Carlo (i.e. no determinism).
- 3) Consideration of the second moment.

Although based on the second moment, many important features (multi-responses, diagnostics, ..... ) may also be incorporated into classical, first moment-based semi-automatic methods.



Out from the core: to decouple or not to decouple

1: Background



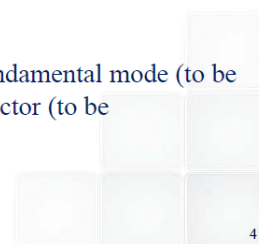
Some 4-5 years ago, we wondered if we could transfer what we had done in fixed source problems to eigenvalue ones. We constrained the eigenvalue problems to those involving the source-iteration algorithm.

The key aspect in applying our variance reduction parameter generator to the source-iteration algorithm is the multi-response capability.

In applying VR to the eigenvalue problem, we are changing the sampling in the fissile zone and in the reflector and thereby distorting the fundamental mode.

But the fundamental mode is the source for the next cycle in which again we are changing the sampling to improve the statistics of local detectors, be they in- or ex-core and logging the fundamental mode, the source for the next cycle, etc.

Clearly there is a trade-off between the amount of distortion of the fundamental mode (to be minimized) and the alteration of the number of tracks at the local detector (to be maximized).



## Out from the core: to decouple or not to decouple

### 2: Problem statement



The problems in eigenvalue calculations that can require variance reduction can be conveniently divided into in-core and ex-core problems.

There are a limited range of in-core problems that may require variance reduction.

Instead ex-core problems nearly always require variance reduction. In this case the normal approach is to decouple the calculation. The point of decoupling is discretionary. It can be the fission sites, the leakage current from the core, ..... We always choose the fission sites.

The paper presented here deals with ex-core problems.

We look to calculate all the ex-core responses in a single eigenvalue calculation employing the source-iteration algorithm, thus avoiding the extra work and the inherent approximations of decoupling.



5

## Out from the core: to decouple or not to decouple

### 3: Methodology



The methodology is described in the following papers:

K.W. Burn, "Optimizing variance reduction in Monte Carlo eigenvalue calculations that employ the source iteration approach", *Ann. Nucl. Energy* **73**, 218 (2014)

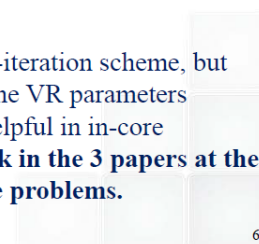
K.W. Burn, "Estimating Local In- and Ex-Core Responses within Monte Carlo Source Iteration Eigenvalue Calculations", Proc. of PHYSOR-2014 (Oct. 2014) and JAERI-Conf 2014-003

K.W. Burn, "A correction and a clarification to 'Optimizing variance reduction in Monte Carlo eigenvalue calculations that employ the source iteration approach'", *Ann. Nucl. Energy* **85**, 776 (2015)

Use is made of "superhistories" (renormalization every  $n$  fission generations):

R.J. Brissenden, A.R. Garlick, "Biases in the Estimation of  $K_{eff}$  and Its Error by Monte Carlo Methods", *Ann. Nucl. Energy* **13(2)**, 63 (1986)

not to mitigate the problem of underestimation of errors in the source-iteration scheme, but rather to improve the variances of local responses (aided by varying the VR parameters according to the fission generation within the superhistory). This is helpful in in-core problems but not in ex-core problems. **The conclusion from the work in the 3 papers at the top of this slide was that we do not need superhistories for ex-core problems.**



6

Out from the core: to decouple or not to decouple  
4: Sample problems



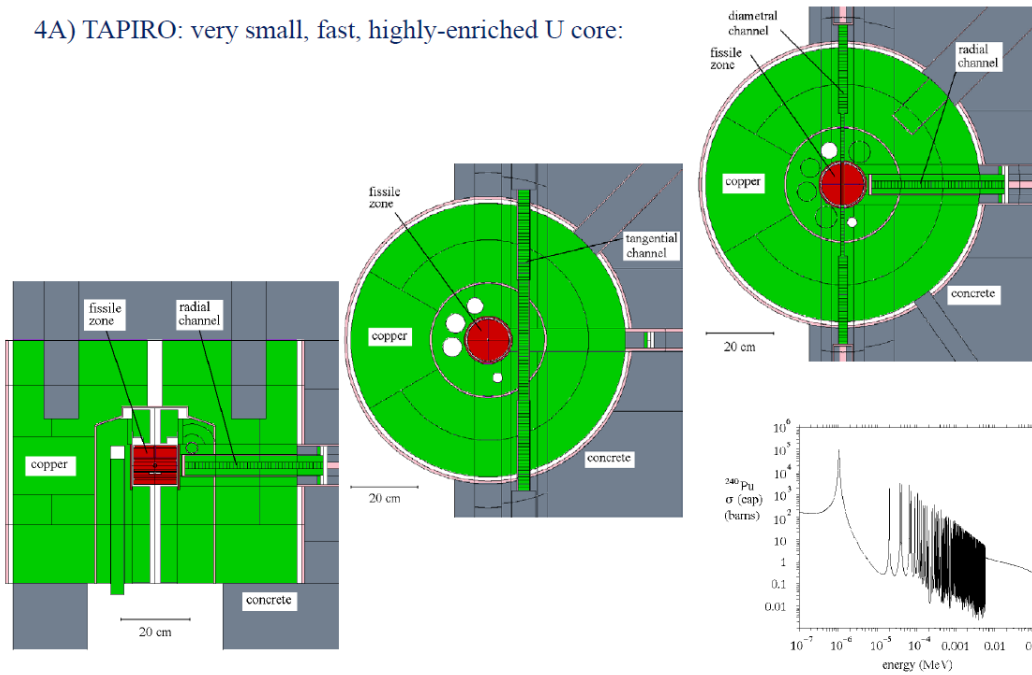
The two contrasting sample problems (small fast core, large thermal core) clarify the previous statements.



Out from the core: to decouple or not to decouple  
4: Sample problems (TAPIRO)



4A) TAPIRO: very small, fast, highly-enriched U core:



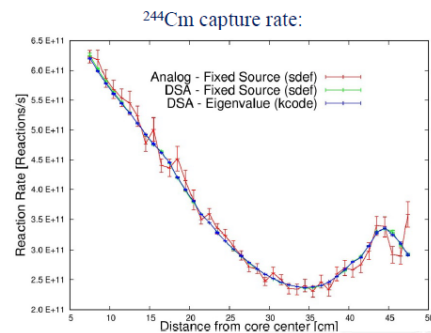
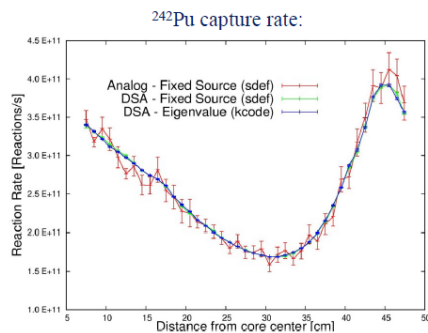
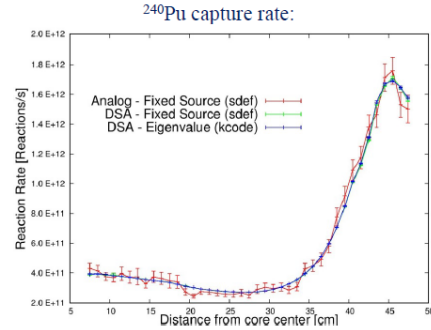
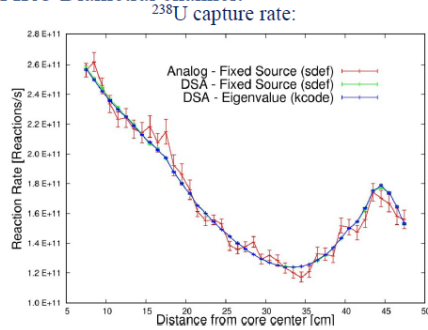


Out from the core: to decouple or not to decouple

4: Sample problems (TAPIRO)



TAPIRO Diametral channel:

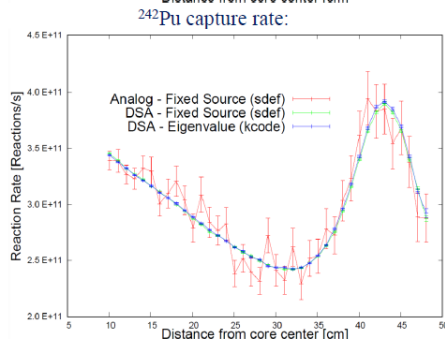
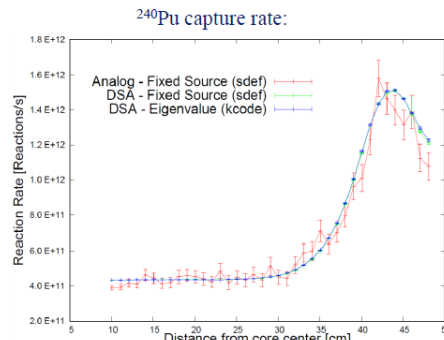
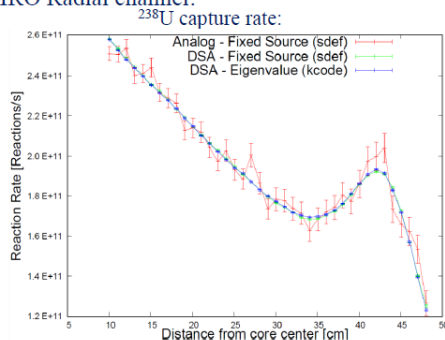


Out from the core: to decouple or not to decouple

4: Sample problems (TAPIRO)



TAPIRO Radial channel:



Out from the core: to decouple or not to decouple

4: Sample problems (TAPIRO)



Conclusions for TAPIRO:

- 1) Decoupled approach is sufficiently accurate (and easy).
- 2) Single eigenvalue calculation approach works well and with 1 fission generation per superhistory (i.e. we do not need superhistories).

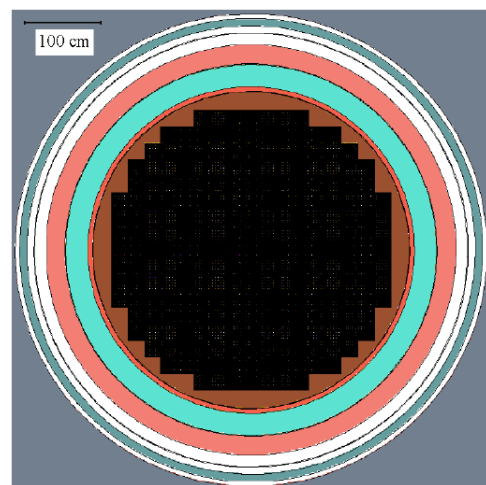
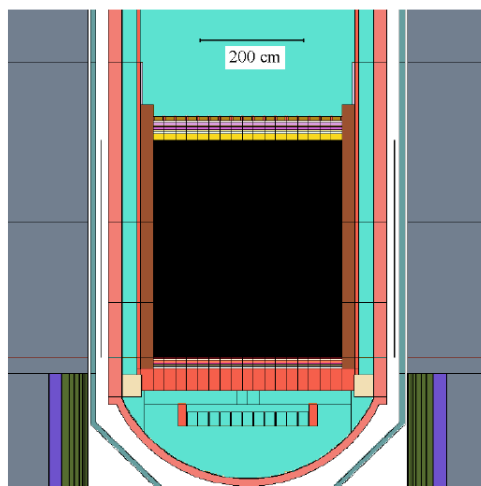


Out from the core: to decouple or not to decouple

4: Sample problems (GEN III PWR)



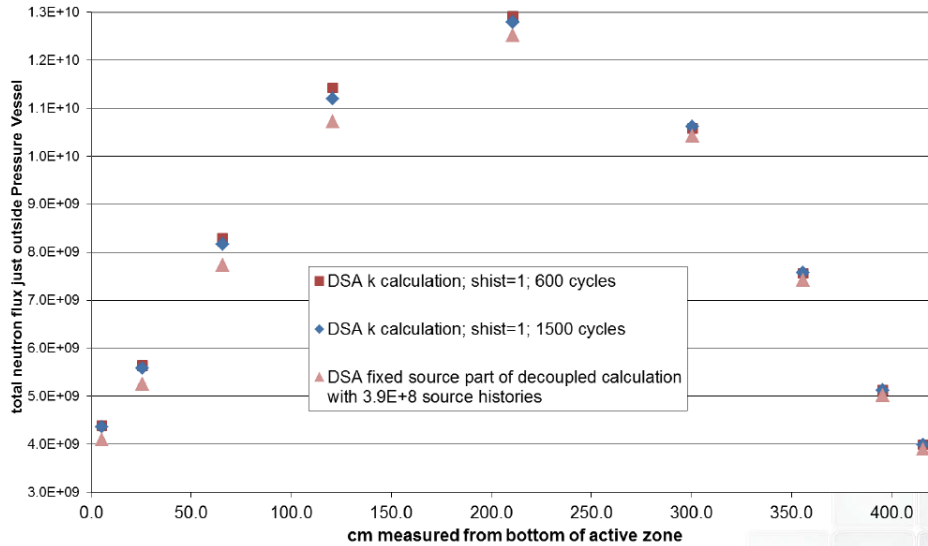
4B) Large size PWR (simplified model):



Out from the core: to decouple or not to decouple  
4: Sample problems (GEN III PWR)



Large size PWR: Axial profiles of the total neutron flux just outside the pressure vessel:



Out from the core: to decouple or not to decouple  
4: Sample problems (GEN III PWR)



First conclusions for large size PWR:

- 1) Decoupled approach with a pin-wise fission source is long and cumbersome (and lowers QA).
- 2) Single eigenvalue calculation approach with 1 fission generation per superhistory produces large scale distortions in the axial flux profiles outside the pressure vessel.

Out from the core: to decouple or not to decouple  
4: Sample problems (GEN III PWR)



What is going wrong for the case: large size PWR?

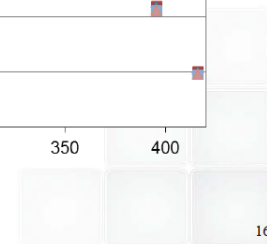
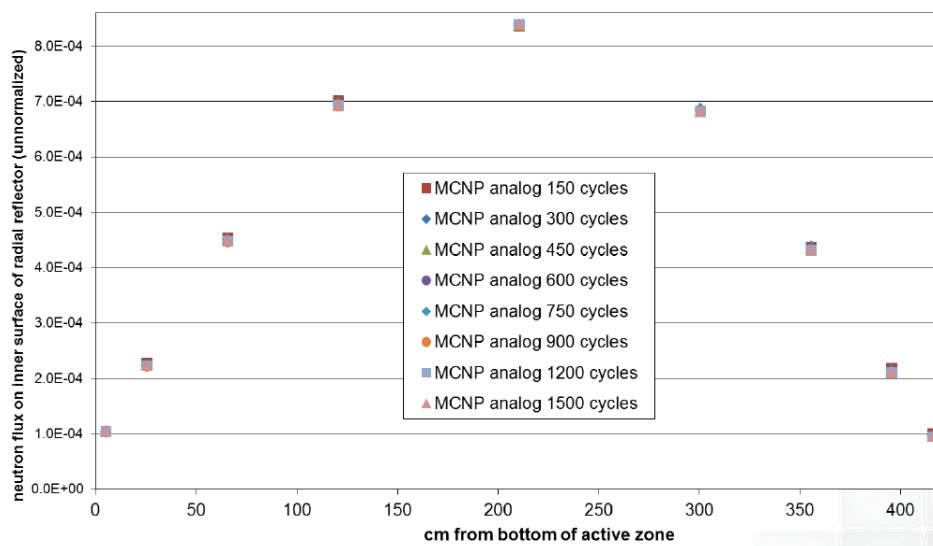
→ look at the axial profile of the core leakage flux.



Out from the core: to decouple or not to decouple  
4: Sample problems (GEN III PWR)



Evolution of axial profile of the core leakage flux with analog MCNP looks like this:

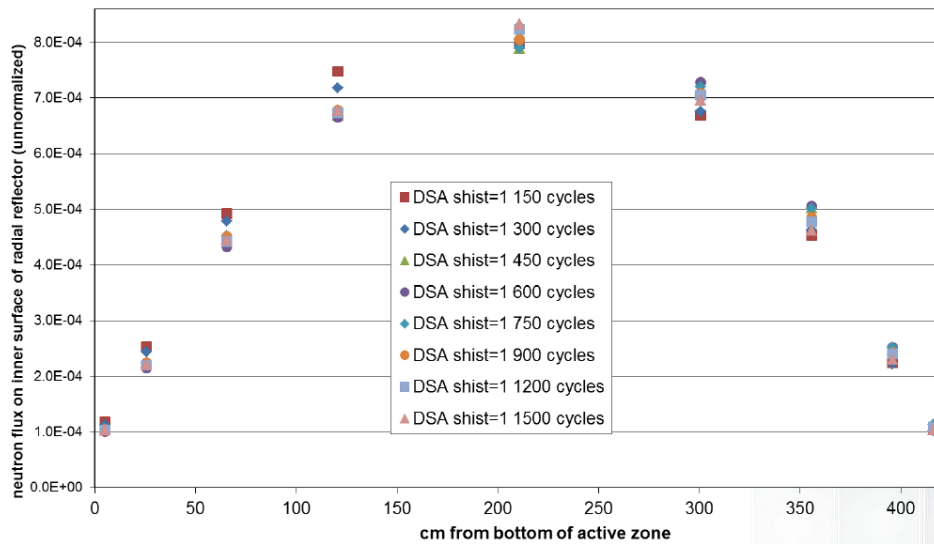


Out from the core: to decouple or not to decouple

4: Sample problems (GEN III PWR)



Evolution of axial profile of the core leakage flux with DSA-optimized importances to 48 ex-core responses and 15 in-core responses and with a superhistory of 1 fission generation looks like this:

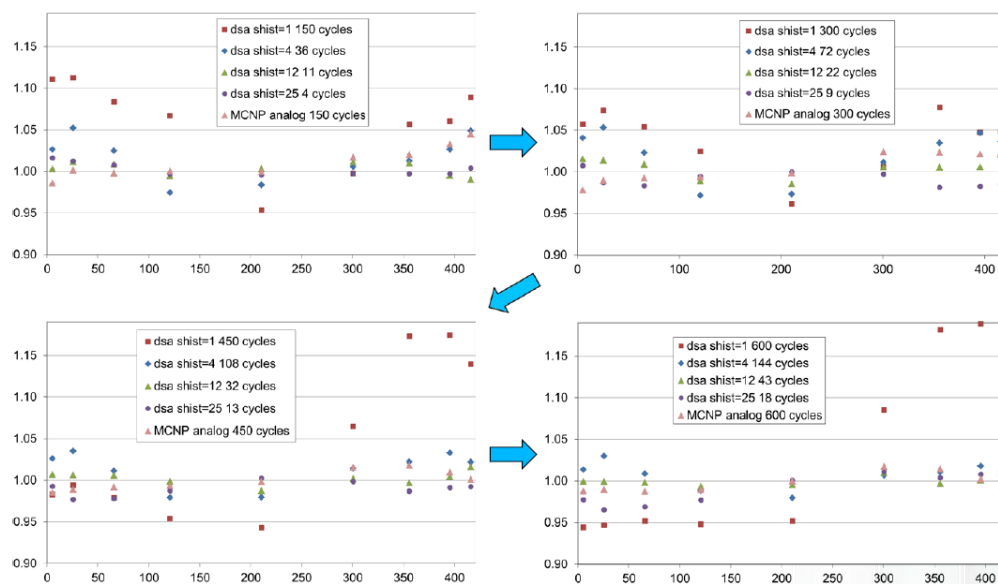


Out from the core: to decouple or not to decouple

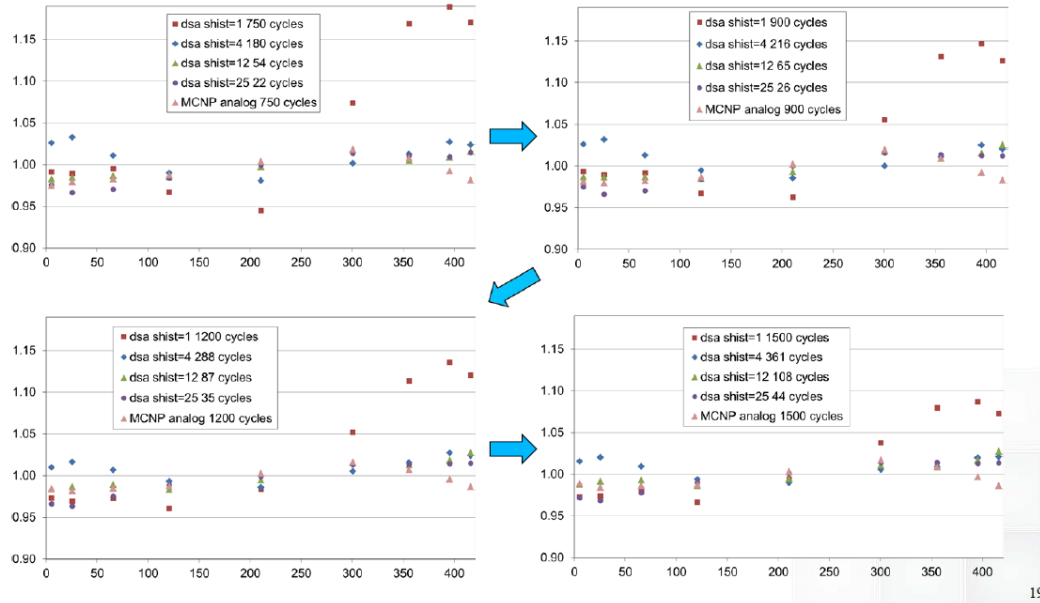
4: Sample problems (GEN III PWR)



Run the same calculation but with superhistories of 4, 12 and 25 fission generations:



Out from the core: to decouple or not to decouple  
4: Sample problems (GEN III PWR)



19

Out from the core: to decouple or not to decouple  
4: Sample problems (GEN III PWR)



Already a superhistory of 4 fission generations is markedly better than 1.

→ It looks as if a superhistory of 10 fission generations should be sufficient to maintain the fundamental mode.

Why?

- 1) Longer in-core transport between normalization points → allows a better settling of the fission distribution.
- 2) Automatically raises the weight attached to the in-core responses (compared with the ex-core ones) due to transmission through the fissions of the response importances in future fission generations within a superhistory.

What do the in-core importances look like for different superhistories?



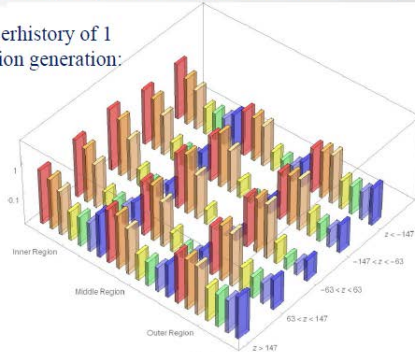
20

Out from the core: to decouple or not to decouple

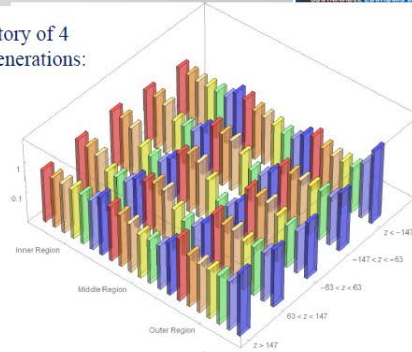
4: Sample problems (GEN III PWR)



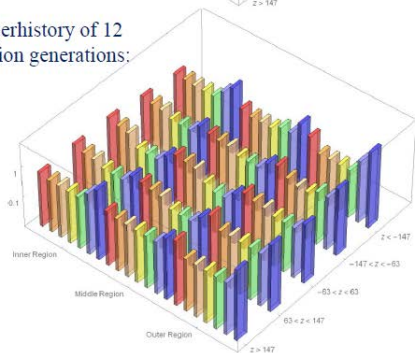
Superhistory of 1 fission generation:



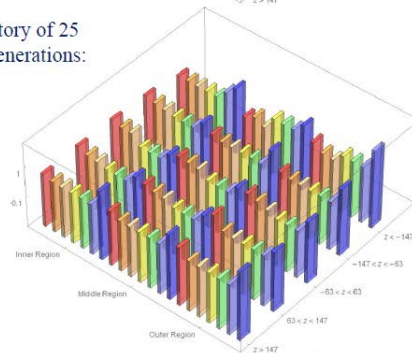
Superhistory of 4 fission generations:



Superhistory of 12 fission generations:



Superhistory of 25 fission generations:



Out from the core: to decouple or not to decouple

5: Conclusions



- To go any distance ex-core you need VR parameters.
- Decoupling may be long, cumbersome and approximate, and may reduce the QA.
- Recently we proposed a way of calculating ex-core responses within the source-iteration algorithm (i.e. without decoupling).
- Here we modify the recommendations from the previous work:

**Always use superhistories of at least 10 fission generations for both in-core and ex-core local responses.**

